- 1 Running Head: Tundra Response to Climate with Grazing
- 2 Model Responses to CO<sub>2</sub> and Warming Are Underestimated without Explicit
- 3 Representation of Arctic Small-Mammal Grazing

- 5 Edward B. Rastetter<sup>1,\*</sup>, Kevin L. Griffin<sup>2, 3, 4</sup>, Rebecca J. Rowe<sup>5</sup>, Laura Gough<sup>6</sup>, Jennie R.
- 6 McLaren<sup>7</sup>, and Natalie T. Boelman<sup>4</sup>
- <sup>1</sup>The Ecosystems Center, Marine Biological Laboratory, Woods Hole, MA 02543, USA
- 8 <sup>2</sup>Department of Ecology, Evolution and Environmental Biology, Columbia University, New
- 9 York, NY 10027, USA
- <sup>3</sup>Department of Earth and Environmental Sciences, Columbia University, Palisades, NY 10964,
- 11 USA
- 12 <sup>4</sup>Lamont-Doherty Earth Observatory, Columbia University, Palisades, NY 10964, USA
- <sup>5</sup>Natural Resources and the Environment, University of New Hampshire, Durham, NH 03824,
- 14 USA
- 15 <sup>6</sup>Department of Biological Sciences, Towson University, Towson, MD 21252, USA
- <sup>7</sup> Department of Biological Sciences, University of Texas at El Paso, El Paso, TX 79968, USA
- <sup>\*</sup>Corresponding author, erastetter@mbl.edu

- 19 Open Research Statement: New empirical data were not used for this research. The code (Rastetter et al.,
- 20 2021a) is available from Zenodo: http://doi.org/10.5281/zenodo.5083290 and the simulation results
- 21 (Rastetter et al., 2021b & 2021c) are available from the Environmental Data Initiative:
- 22 https://doi.org/10.6073/pasta/67108cef344d93cfdd060e7e0f0911f5 and
- 23 <u>https://doi.org/10.6073/pasta/42e6660b2d1f2b59985ed0940e53f0d4.</u>

# **ABSTRACT**

We use a simple model of coupled carbon and nitrogen cycles in terrestrial ecosystems to examine how explicitly representing grazers versus having grazer effects implicitly aggregated in with other biogeochemical processes in the model alters predicted responses to elevated carbon dioxide and warming. The aggregated approach can affect model predictions because grazer-mediated processes can respond differently to changes in climate from the processes with which they are typically aggregated. We use small-mammal grazers in arctic tundra as an example and find that the typical three-to-four-year cycling frequency is too fast for the effects of cycle peaks and troughs to be fully manifested in the ecosystem biogeochemistry. We conclude that implicitly aggregating the effects of small-mammal grazers with other processes results in an underestimation of ecosystem response to climate change relative to estimations in which the grazer effects are explicitly represented. The magnitude of this underestimation increases with grazer density. We therefore recommend that grazing effects be incorporated explicitly when applying models of ecosystem response to global change.

**KEYWORDS:** arctic tundra, biogeochemistry, carbon cycling, carbon-nitrogen ecosystem model, climate change, nitrogen cycling, population cycles, small-mammal herbivores

#### INTRODUCTION

42

43

44

45

46

47

48

49

50

51

52

53

54

55

56

57

58

59

60

61

62

63

64

Despite evidence that animals can influence ecosystem carbon (C) and nutrient cycles (Schmitz et al., 2014), explicit incorporation of animals into terrestrial biogeochemical models is rare (Metcalfe and Olofsson 2015). To maintain mass balance in these models without explicit representation of animals, the effects of animals have to be implicitly aggregated into other biochemical processes though model calibration (e.g., animal respiration included with other heterotrophic respiration). However, animal-mediated processes can behave differently from the processes with which they are aggregated. For example, combining microbial and mammal respiration into a single value for heterotrophic respiration can cause problems because warming generally increases respiration in microbes, but can slow respiration in mammals if the warming reduces the energy needed to maintain body temperature (Batzli et al., 1980). Here we examine the effects of aggregating grazer-mediated processes in with other biogeochemical processes when modeling ecosystem response to elevated carbon dioxide (CO<sub>2</sub>) and warming. We use small-mammal grazers in arctic tundra as an example. However, the principles are general, and we conclude with a discussion of how our results might apply more generally to other grazers and other ecosystems. Recent studies suggest that animals influence the response of tundra to climate change (Tuomi et al., 2019, Petit Bon et al., 2020). Experimental manipulations conducted across a range of tundra ecosystems have shown that while warming or fertilization typically enhances above ground productivity and nutrient cycling in tundra, the presence of herbivores - including rodents, geese, and ungulates - can dampen or negate this response (e.g., Grellman et al., 2002, Sjögersten et al., 2008, Post and Pedersen 2008, Rinnan et al., 2009, Cahoon et al., 2011,

Kaarlejärvi et al., 2015, Leffler et al., 2019) or might enhance productivity (Gough et al., 2012).

Further, observational studies have shown that trophic interactions on the tundra strengthen under warmer conditions (McKinnon et al., 2010, Legagneux et al., 2012), suggesting that animal influences on arctic C cycling might be stronger in the future.

In other terrestrial ecosystems, animals are known to affect C and nutrient cycling (McNaughton 1985, McLaren and Jefferies 2004, Wilkinson and Sherratt 2016). The direct effects of animals vary among ecosystems, type of herbivore, and plant growth form (Jai et al. 2018) but have historically been thought of as small relative to plant and microbial processes (e.g., Hairston et al., 1960). Nevertheless, animals can accelerate nutrient cycles and influence plants and microbes indirectly by mediating chemical and biological processes and altering community structure and can thereby have a large influence on ecosystem C and nutrient processing (Pastor et al., 1988, Schmitz et al., 2014, Wardle et al., 2004, Zimov et al., 2009, Metcalfe et al., 2014).

Although herbivore-vegetation models have been made for other ecosystems (e.g., Seagle and McNaughton 1993, Bennett 2003), we are aware of only one vegetation-dynamics model - ArcVeg - that explicitly addresses the effect of an arctic herbivore (caribou) on tundra biogeochemistry (Yu et al., 2011). This model indicates that grazing dampens the increase in plant biomass expected from warming soils and the consequent increase in nutrient cycling (Yu et al., 2011). These results suggest that the explicit inclusion of grazers in biogeochemical models could be necessary for predicting tundra responses to climate change.

Other modeling studies have addressed arctic biogeochemical responses to climate change, but without the explicit representation of the effects of animals as separate from other C and nutrient cycling processes. These biogeochemical models indicate significant long-term impacts of elevated CO<sub>2</sub> and warming, but the model predictions differ on how these responses

will ultimately affect net C source versus sink activity. This source-sink disparity is due to uncertainty in the balance between elevated autotrophic and heterotrophic respiration (source) resulting from warming versus enhanced photosynthesis (sink) resulting from the direct effects of elevated CO<sub>2</sub> and warming on production and from the acceleration of nutrient cycles by warming (McKane et al., 1997, Rastetter et al., 1997, McGuire et al., 2012, Pearce et al., 2015, Jiang et al., 2017). This trade-off between source versus sink activity is likely to be confounded by arctic herbivores.

From the perspective of ecosystem biogeochemistry, aggregating herbivore effects in with other processes can be justified because grazers perform several nutrient-cycling processes that parallel other plant and microbial processes within ecosystems. Here we examine aggregation effects for four such processes in relation to the response of ecosystems to elevated CO<sub>2</sub> and warming: (1) Grazing mediates the transfer of plant C to detritus and soil organic matter (soil), and thereby acts in parallel with tissue senescence and litter fall. (2) Similarly, grazing transfers plant N to soil organic matter in parallel with tissue senescence and litter fall, but does so before the plants can resorb N. (3) Consumption of plant material and subsequent heterotrophic respiration by grazers parallels litter fall and the subsequent heterotrophic respiration resulting from processing of soil organic matter by microbes and other detritivores. (4) Finally, metabolic processing of plant matter consumed by grazers produces dissolved labile N in urine in parallel with litter fall and microbially mediated mineralization.

Even though these processes act in parallel, the grazer-mediated and non-grazer-mediated processes might respond differently to climate change, or even in opposite directions.

Furthermore, the cyclic dynamics of small-mammal grazers in the Arctic might complicate the

relative contributions of these parallel processes to ecosystem responses to elevated CO<sub>2</sub> and climate change. Based on the modeling analysis we present below:

- (1) We hypothesize that aggregating the effects of small-mammal grazers with other C and N cycling processes results in an underestimation of tundra responses to elevated CO<sub>2</sub> and warming. For our model, after 100 years the underestimation of C sequestration in tundra ecosystems in response to elevated CO<sub>2</sub> and warming is 50 to 80% relative to estimations in which the grazer effects are explicitly represented.
- (2) We hypothesize that although three-to-four-year cycles in the density of small-mammal grazers have measurable short-term effects of tundra biogeochemistry (e.g., Olofsson et al. 2012), densities averaged over the grazer cycles can be used to assess long-term responses of tundra to elevated CO<sub>2</sub> and warming.

We use a simple model of coupled C and N cycles in ecosystems applied to the effects of small-mammal grazers on the responses of moist acidic tundra to elevated CO<sub>2</sub> and warming. Most of the data we use is for lemmings and voles, but the model applies to generic small-mammal grazers in the Arctic, which we refer to as "voles" for simplicity. We apply the model both with vole densities explicitly represented and with vole densities unspecified, but their effects implicitly subsumed into other biogeochemical processes. In all applications of the model, we assume voles are present on the landscape. The model applications differ only in the way that vole and other biogeochemical processes are separated from one another.

# **METHODS**

**Model:** We use a model developed by Rastetter et al., (2020) to examine recovery of ecosystems from disturbances that remove vegetation (Box 1). We have modified that model to account for temperature sensitivity of six metabolic processes (photosynthesis, autotrophic and heterotrophic respiration, plant and microbial N uptake, and N mineralization). We have also modified it to account for the effects of voles on the transfer of C and N from vegetation to soil organic matter and the transfer of N in urine from vegetation to inorganic N (although not all N in urine is inorganic, it is labile, and we treat it as inorganic). The basic model is fully described in Rastetter et al., (2020); here we describe only the changes to that model for the current analyses.

Temperature response of metabolic processes: Because we use an annual time step in the model (i.e., no seasonality) and restrict warming to 5 °C above current temperatures, we use a simple Q<sub>10</sub> function to simulate temperature responses rather than more complex formulations (e.g., Heskel et al., 2016 or Carey et al., 2016). We have therefore modified the photosynthesis, autotrophic respiration, heterotrophic respiration, plant N uptake, microbial N uptake, and N mineralization in the Rastetter et al., (2020) model to increase exponentially with warming (Box 1: Eqs. 9, 10, 13, 14, 19, and 20).

Vole grazing: We drive the model by specifying vole density in each year (V).

Consistent with values and cycle frequency reported in the literature (Batzli et al., 1980, Krebs et al., 1995, Korpimaki et al., 2004, Pitelka and Batzli 2007, Krebs 2013, Ehrich et al. 2020), we use a randomly generated time series of vole abundance with peaks every three or four years, with abundances at the peak ranging from 90 to 110 voles ha<sup>-1</sup>, minimum abundances ranging from 8 to 12 voles ha<sup>-1</sup>, and a mean vole abundance over the full time series of 40 voles ha<sup>-1</sup> (Fig. 1). We chose to take this prescribed approach to vole density because the drivers of vole cycles

are not fully understood (Korpimaki et al., 2004, Prevedello et al., 2013, Oli 2019) and likely include a top-down component (Pitelka et al., 1955, Hairston et al., 1960, Krebs 2013), which is well beyond the domain of our model. For convenience, we specify vole density in voles ha<sup>-1</sup> and correct to m<sup>-2</sup> units by dividing by 10,000 m<sup>2</sup> ha<sup>-1</sup> (Eqs. 15, 17, & 18).

The removal of C from vegetation for nest building and ingestion are lumped into a single process for our model (Eq. 15). We assume this C removal is proportional to the specified vole density but decrease the per capita rate of ingestion with warming to account for decreased energy requirements to maintain body temperature (Eq.15; Batzli et al., 1980). Vole respiration is proportional to the ingestion component of C removal from vegetation by voles and therefore also declines with warming (Eq. 17). We do not account for other temperature responses like those associated with cold or heat stress. We assume a constant C:N ratio of material removed from vegetation by grazers (Eq. 16) but, because of the respiration loss of C and the N transferred to inorganic N in urine, the C:N of material removed from vegetation and the C:N of material added to the soil organic matter differ. Finally, we assume urine losses of N are proportional to vole density (Eq. 18).

Model calibration: We calibrate the model to be consistent with the C and N stocks and process rates compiled by Pearce et al., (2015) for the Multiple Element Limitation (MEL) model (Table 1). Because voles are part of the ecosystem, the effects of voles on tundra C and N stocks and fluxes are implicitly included in the data compiled by Pearce et al., (2015). Therefore, by using these data to calibrate (fit) the model without explicit vole representation, we are implicitly aggregating those vole effects in with the parallel ecosystem processes described above. In the calibrations in which voles are explicitly represented, we

assume a constant vole density and that the ecosystem is in steady state. We then specify the vole effects directly and subtract these effects from the parallel ecosystem processes before calibration (Table 2). The combined rates of vole-mediated processes plus the parallel ecosystem processes are therefore identical in all calibrations (rows labeled "Total" in Table 2), thus providing the basis of comparison for assessing the consequences of explicit versus aggregated representation of vole grazing.

In the calibrations, first we set allometric, C:N, Q<sub>10</sub>, half-saturation, and vole-related parameters (derivation of these parameter values is presented in Appendix S1). We then set the rate parameters for each process so that flux rates are consistent with rates reported in Pearce et al., (2015). Because annual rates of plant and microbial processes are dominated by growing-season rates, we use average summer temperature (10 °C) to calibrate the model; in any case, because of the Q<sub>10</sub> formulation, once calibrated to a specified temperature, model responses are sensitive to changes in temperature, not to the temperature value itself. For vole processes, we correct this summer temperature to average annual temperature with an off-set (Eq. 15).

We made three calibrations (Tables 3 & 4). In calibration I, vole densities are not explicitly specified, and we assume that vole-mediated processes can be implicitly represented by aggregating them with the parallel biogeochemical processes described in the introduction above (Table 2). In this calibration, we therefore set the number of voles (V) in the model to zero but incorporate the effects of voles in with the parallel processes through the calibration. In calibration II, we set the number of voles to 40 voles ha<sup>-1</sup> so that vole-mediated processes are explicitly represented, and the number of voles is the mean abundance of voles we use in our simulated vole cycle (described above). In calibration III, we set the number of voles to 100 voles ha<sup>-1</sup>, which is the mean peak-vole abundance in our simulated vole cycle. In calibration

III, the parallel ecosystem process rates are decreased proportionally more than in calibration II to account for the higher vole density (Table 2).

All but four of the parameters have the same values in all three calibrations. To maintain the same steady state in all three calibrations, we adjust the values of these four parameters to compensate for how voles are represented in the model ( $m_{CB}$ ,  $m_{NB}$ ,  $r_{D}$ , and  $m_{Nm}$ ; rows labeled "PAR" in Table 2). These parameters are adjusted so that the rates of C and N litter losses, heterotrophic soil respiration, and gross N mineralization all decrease to compensate for the parallel vole-mediated C and N fluxes in calibrations II and III where voles are explicitly represented. Because we calibrate to the same data set (Pearce et al., 2015), the overall C and N stocks and cycling rates are identical for these three calibrations (rows labeled "Total" in Table 2).

**Simulations:** We run a total of thirteen simulations in two sets (Tables 3 & 4).

In the first set of simulations, we assume that the average vole density is 40 voles ha<sup>-1</sup> and use calibration II with vole effects explicitly represented (Table 3). We then run four 200-year simulations with no change in either CO<sub>2</sub> or temperature. We drive the model with: (1) voles held constant at 40 voles ha<sup>-1</sup>; (2) voles cycling on the three-to-four-year cycle between 8 and 110 voles ha<sup>-1</sup> for 200 years; (3) voles cycling for ten years, followed by maintenance of a constant vole density of 100 voles ha<sup>-1</sup> (equivalent to adding voles to the ecosystem); and (4) voles cycling for ten years, followed by maintenance of a constant vole density of 0 voles ha<sup>-1</sup> (equivalent to removing voles from the ecosystem).

This first set of simulations serves two purposes. First, it illustrates the effects of longterm changes in vole density and thereby draws the distinction between adding or removing voles from calibrating the model assuming high or low vole density. Second, it allows us to assess the potential long-term effects of voles if their numbers were maintained at high or low levels. We can thereby address the question: "Do the simulated changes in the ecosystem approach their potential changes during peaks and troughs in the vole cycle?"

The second set of simulations is to address our central question about aggregated versus explicit representations of grazer effects on ecosystem responses to climate change (Table 4). We run nine 100-year simulations in a two-factor design. The first factor relates to how vole effects are represented in the three calibrations (Table 3) and vole abundance: (1) calibration I (aggregated) and vole abundance subsumed in the calibration of the parallel processes and therefore assumed constant but unspecified (although V is set to 0 in the model, vole effects are aggregated in with the parallel ecosystem processes); (2) calibration II (40 voles ha<sup>-1</sup>) and vole abundance cycling on the three-to-four-year cycle between 8 and 110 voles ha<sup>-1</sup>; and (3) calibration III (100 voles ha<sup>-1</sup>) and vole abundance held constant at 100 voles ha<sup>-1</sup>. The second factor relates to climate change: (1) a linear increase in atmospheric CO<sub>2</sub> from 400 to 800 μmol mol<sup>-1</sup> over 100 years; (2) a linear increase in temperature from 10 to 15 °C over 100 years; and (3) a linear increase in both atmospheric CO<sub>2</sub> from 400 to 800 μmol mol<sup>-1</sup> and temperature from 10 to 15 °C over 100 years.

# **RESULTS**

# Set 1: Effects of vole cycling and adding or removing voles.

Simulation 1: Effects of holding voles constant at the calibration abundance. Because the model was calibrated to a steady state with 40 voles ha<sup>-1</sup>, all ecosystem C and N stocks and fluxes remained constant when vole abundance was held at 40 voles ha<sup>-1</sup> in the 200 year

simulations (dotted horizontal lines in Fig. 2). This simulation only serves to illustrate the stability of the model and to serve as a control to which the other simulations can be compared.

Simulation 2: Effects of vole cycling on plant and soil C and N. In the 200-year simulations with vole abundance cycling, the plant and soil C and N stocks cycle at the same three-to-four-year frequency as the voles (Fig. 2). In addition, there are some longer-term dynamics in these stocks associated with the auto-correlated nature of plant production and the legacy of the random variations in the vole cycle. Despite these dynamics, vole cycling does not cause the plant and soil C and N stocks to diverge far from the values to which they are calibrated (dotted and solid lines in Fig. 2).

The plant biomass cycles out of phase with the vole cycle. The lowest plant C and N values occur in years of peak vole numbers and the highest plant C and N values occur three or four years after peak vole numbers or the year prior to the subsequent vole peak (Fig. 3). This phase shift in the plant relative to vole cycles as well as the magnitude of the plant C cycle (20 to 30 g C m<sup>-2</sup> peak to trough) are roughly consistent with the phase and magnitude of the cycles reported by Olofsson et al., (2012). In addition, the dependence of plant production on plant biomass results in a strong autocorrelation in the plant C and N time series, which in turn results in longer-term dynamics less clearly tied to the vole cycle (Fig. 2). This autocorrelation is reflected in the strong positive correlation between the plant C and N and their respective values at the time of the previous peak in vole numbers (open dots remain high and closed dots remain low in Fig. 3).

The dynamics of soil C and N stocks are closely tied to the plant dynamics. Because N inputs to the ecosystem are less than 3% of the annual plant requirement (Table 1), plant recovery from vole outbreaks relies almost exclusively on N from soil organic matter. As a

consequence, the three-to-four-year soil N cycles are directly out of phase with plant N cycles and the longer-term dynamics are also opposite those in plant N (Fig. 2). Soil C also cycles out of phase with plant C, but the relation is not as strong as it is for N. However, because soil C is ultimately derived from plant C, the longer-term dynamics in plant C are paralleled in the soil C following about a 9-year lag (Fig. 2).

Simulations 3 & 4: Effects of removing or adding voles. When voles are removed from the ecosystem, plant C and N increase by about 13%, or increase by 116 g C m<sup>-2</sup> and 2.7 g N m<sup>-2</sup>. Because of the reliance of plants on soil N, soil N deceases by almost the same absolute amount as the plants gain, 2.5 g N m<sup>-2</sup>. However, the amount of N in the soil is so large that this loss amounts to only about a 0.3% loss. The increase in plant biomass results in higher litter inputs to the soil. Consequently, soil C increases by about 4% or 727 g C m<sup>-2</sup>. The gain of soil C and loss of soil N widens the soil C:N ratio by about 4%, which in turn increases microbial N immobilization into soil organic matter (effect of Φ in Eq. 14).

When voles are increased and then held constant at 100 voles ha<sup>-1</sup>, plant C and N decrease by about 20%, or 175 g C m<sup>-2</sup> and 4 g N m<sup>-2</sup>. Again, because of the tight cycling of N in the ecosystem, soil N increases by almost the same absolute amount as the plants lose, 3.7 g N m<sup>-2</sup> (0.4%). The loss of plant biomass translates into lower litter inputs to soil and a large absolute decrease in soil C, 1170 g C m<sup>-2</sup> (6%). Because of the increase in soil N and decrease in soil C, the soil C:N narrows by about 6%, which in turn decreases microbial N immobilization into soil organic matter (effect of Φ in Eq. 14).

In the simulations where vole density is increased or decreased and then held constant, it takes 10 to 20 year for the vole effects to reach their largest deviation from the steady state and another 60 to 90 years for those effects to stabilize. Because of this long response time, the

potential effects of voles on tundra biogeochemistry cannot be approached if vole abundance cycles on a three-to-four-year cycle. Indeed, when voles are cycling, the magnitude of these effects relative to the peak effects of the long-term increase or decrease in vole abundance is only about 12% for plant C, 2% for soil C, and 20% for both plant and soil N.

# Set 2: Effects of aggregated versus explicit representations of vole effects.

Simulations 5, 8, & 11: Responses to increasing CO<sub>2</sub>. Predicted responses to increased CO<sub>2</sub> do not differ substantially between the aggregated model in which vole effects are implicitly aggregated in with other biogeochemical processes through model calibration (calibration I) and the distributed model in which vole effects are explicitly represented (calibrations II & III: Figs. 4, 5, & 6). The only process affected by elevated CO<sub>2</sub> is photosynthesis. However, because the plants are strongly N limited, elevated CO<sub>2</sub> increases net primary production (NPP) by only 10-11% in both aggregated and distributed simulations (Fig. 6). This increase in production translates into about an 11-12% increase in biomass, again in both aggregated and distributed simulations (Fig. 4). The increase in production results in only about a 4% increase in soil C in all the simulations. This increase in soil C is a small relative change but, because soil has such a large fraction of the organic matter, it is a large absolute change amounting to about 90% of the total change in ecosystem C.

The amount of N entering the ecosystem is too small to support even the small gain in plant C in response to elevated CO<sub>2</sub>. The gain is instead supported by a net transfer of 0.9 - 1.3 g N m<sup>-2</sup> from soil to plants over the 100-year simulations. The amount of N transferred from soil to plants is about the same in all three simulations (Fig. 5). Elevated CO<sub>2</sub> increases the C:N ratio of the plants, which in turn increases N uptake (effect of  $\Psi$  in Eq. 10). However, the increase in soil C:N resulting from increased litter inputs also increases microbial N uptake (effect of  $\Phi$  in

Eq. 14). This competition between plants and microbes for N limits the ecosystem response to elevated CO<sub>2</sub>. Again, the effects of aggregated versus explicit representation of voles on this response to elevated CO<sub>2</sub> are negligible (Figs. 4, 5, & 6).

316

317

318

319

320

321

322

323

324

325

326

327

328

329

330

331

332

333

334

335

336

337

338

Simulations 6, 9, & 12: Responses to warming. In contrast, the effects of aggregated versus explicit representation of voles on the response to warming are large (Figs. 4, 5, & 6). Warming not only stimulates photosynthesis, it also stimulates autotrophic and heterotrophic respiration, and, more importantly, it stimulates the N cycle in three places: (1) N mineralization, (2) microbial N uptake, and (3) plant N uptake. A major effect of this stimulation of the N cycle is an increase in net N mineralization, a resulting relaxation of N limitation on plant growth, and a large increase in plant biomass. The increase in plant production increases litter inputs to soils, which in turn mitigates soil C losses. In addition, the increased production allows the ecosystem to accumulate a small amount of N (<0.3 g N m<sup>-2</sup>; Fig. 6). The effects of this chain of events are much stronger in the simulations where voles are explicitly represented than in the simulations with the aggregated model and the effects are stronger when the model is calibrated assuming higher vole densities (response stronger for calibration III [100 vole ha<sup>-1</sup>] than for calibration II [40 voles ha<sup>-1</sup>]). Thus, explicit representation of vole effects results in an amplification of the predicted transfer of N from soil to plants, larger predicted gains in plant C or higher predicted retention of soil C, and higher predicted rates of gross primary production (GPP), net primary production (NPP), and net ecosystem production (NEP). If the simulations are run with vole density held constant at 40 voles ha<sup>-1</sup>, the C and N stocks and fluxes follow the same general patterns as in the simulations with the three-to-four-year vole cycle (data not shown). The size of the differences between the simulations with constant 40 voles ha<sup>-1</sup> and cycling vole density are about the same as those of the cycle simulation from the steady state with no climate change

(Fig. 2). In addition, the temperature effects on vole consumption and respiration (Box 1, Eqs. 15 & 17) have only a small effect on this general pattern (simulations rerun with  $\varepsilon_V = 0$  resulted in < 2% difference in C and N stocks; data not shown).

Simulations 7, 10, & 13: Responses to increasing CO<sub>2</sub> and warming. The effects of elevated CO<sub>2</sub> and warming are slightly amplified when the two are combined (the two interact synergistically). Under both elevated CO<sub>2</sub> and warming, GPP is 12% and NPP is 8% higher than the sum of the changes in GPP and NPP under elevated CO<sub>2</sub> alone and warming alone (Fig. 6). The net transfer of N from soil to plants is about 3% stronger and the increase in plant C is about 7.5% stronger (Fig. 4 & 5). Overall, because the response to CO<sub>2</sub> alone is so much smaller that the response to warming alone, the response to the two combined is dominated by the warming response. The consequences of aggregated versus explicit representations of vole effects are therefore the same as in the warming simulations.

In our analysis we assume vole density is top-down controlled and therefore does not increase with plant production. However, if the average vole density during the cycle increases in proportion to NPP (~80% over 100 years), some of the increased production with elevated CO<sub>2</sub> and warming is consumed and the increase in plant biomass is about 7.6% lower than when the average vole density remains constant (data not shown). The increase in vole density causes soil C to decrease by 0.9% rather than increase by 0.4%.

# **DISCUSSION**

Our analysis indicates that failure to explicitly represent small-mammal grazers (voles) in biogeochemical models can result in an underestimation of the response of arctic ecosystems to climate warming but has only a small effect on the response to elevated CO<sub>2</sub> (Fig. 4, 5, & 6).

Underestimation of the warming response increases with the assumed density of voles used to calibrate the model. Although cycling of vole density has short-term effects on ecosystem stocks and fluxes, it neither amplifies nor dampens the underestimation in the long-term response to warming. Why is the explicit representation so important?

362

363

364

365

366

367

368

369

370

371

372

373

374

375

376

377

378

379

380

381

382

383

384

Before addressing this question, we again emphasize the distinction between explicit representation of voles and adding voles to the ecosystem. Adding voles to the ecosystem accelerates nutrient cycling by increasing the transfer of nutrients from plants to soil. Such an acceleration of nutrient cycling might be expected to increase the responsiveness to elevated CO<sub>2</sub> and warming. However, in our analysis of the response to elevated CO<sub>2</sub> and warming we do not add voles; we simply change how the voles are represented in the model. Vole effects are either implicitly aggregated in with other processes or they are explicitly represented. In all three of our calibrations, the total amounts of C and N removed from vegetation, the total heterotrophic respiration, and the total mineralization of N are identical (Table 2). Thus, the magnitudes of vole-mediated processes plus the parallel ecosystem processes are represented identically in all three calibrations. Furthermore, in the analysis where we did add voles, any acceleration of nutrient cycles by vole activity is transient; our analysis indicates that the net effect of adding voles is to transfer N from plants, with relatively high N turnover, to soil, with slower N turnover (Fig. 2); although it would be impossible to detect the 0.6% change in soil N predicted by our model. Thus, the long-term effect of adding voles is to slow the nutrient cycle. Furthermore, adding and maintaining 100 voles ha<sup>-1</sup> resulted in a loss of over a kilogram of C from the ecosystem (Fig. 2). Thus, the effect of adding grazers is to decrease ecosystem C whereas explicitly representing voles in the model is to *increase* the estimate of C gain with climate change (Fig. 4).

386

387

388

389

390

391

392

393

394

395

396

397

398

399

400

401

Why are the differences in responses to elevated CO<sub>2</sub> so small between aggregated versus explicit representation of vole effects? Elevated CO<sub>2</sub> stimulates only one ecosystem process, photosynthesis (Fig. 7). The associated increase in C gain increases biomass and leaf area, which further stimulates photosynthesis (Fig. 7:  $\uparrow C_a \rightarrow \uparrow P_s \rightarrow \uparrow B_C \rightarrow \uparrow S \rightarrow \uparrow P_s$ ). However, there is a much stronger negative feedback associated with the change in stoichiometry; increased photosynthesis increases biomass C and consequently increases vegetation C:N, which feeds back to decrease photosynthesis ( $\uparrow C_a \rightarrow \uparrow P_s \rightarrow \uparrow B_C \rightarrow \uparrow \Psi \rightarrow \downarrow P_s$ ). Tissue and Oechel (1987) used this stoichiometric feedback to argue why tussock tundra exposed to elevated CO<sub>2</sub> alone had only a transient increase in production. Without an increase in the N supply to vegetation, the CO<sub>2</sub>-stimulation of photosynthesis cannot be maintained. However, the increase in vegetation C:N increases the litter-fall C:N and consequently the soil C:N, which in turn decreases net N mineralization and the supply of N to plants ( $\uparrow C_a \rightarrow \uparrow P_s \rightarrow \uparrow B_C \rightarrow \uparrow \Psi \rightarrow \uparrow \Psi$  $\downarrow L_{\rm itN} \rightarrow \downarrow D_{\rm N} \rightarrow \uparrow \Phi \rightarrow \downarrow (N_{\rm min} - U_{\rm Nm})$ ). Because none of the steps in this chain were modified to incorporate voles explicitly in the model calibration, this N feedback is about the same for both explicit and aggregated representation of voles in the model and therefore does not have a large effect on the relative responses with and without explicit representation of vole effects.

402

403

404

405

406

407

Why are the predicted responses to warming stronger when vole effects are explicitly represented in the model than when they are aggregated with other processes? In the model, warming stimulates six processes: photosynthesis, autotrophic and heterotrophic respiration, N mineralization, microbial N uptake, and plant N uptake (Fig. 7). Although warming decreased the energy cost of thermoregulation and therefore decreases vole

consumption of plants (Eq. 15) and vole respiration (Eq.17), we found that this effect is too small to explain the differences between simulations with versus without voles explicitly represented (accounting for < 2% of the response in C and N stocks).

Among these many effects of warming in the model, the main effect that results in the accumulation of plant C in simulations with both explicit and aggregated representations of vole effects is the release from N limitation through the stimulation of net N mineralization (Fig. 7:  $\uparrow T \rightarrow \uparrow (N_{\text{min}} - U_{\text{Nm}}) \rightarrow \uparrow N \rightarrow \uparrow U_{\text{N}} \rightarrow \uparrow B_{\text{N}} \rightarrow \downarrow \Psi \rightarrow \uparrow P_{\text{s}}$ ). Thus, one effect of this mobilization of soil N is for both C and N uptake by plants to increase, causing plant biomass to accumulate. Because N mineralization ( $N_{\text{min}}$ ) was decreased in calibrations II and III to accommodate the explicit representation of voles (Table 2), this warming-induced growth in plant biomass is about 0.8% (40-vole calibration II) to 2% (100-vole calibration III) weaker in the simulations with the explicit representation of vole effects. These simulations nevertheless accumulate more, not less, biomass.

The main reason that plant C and N accumulation differed between simulations with aggregated versus explicit representations of voles is the change made to litter fall rates to accommodate the voles in calibrations II and III (Table 2). Litter fall is not directly stimulated by warming (Eqs. 11 & 12), but it does increase as plant biomass increases. This increase in litter fall in turn limits the amounts of C and N that can accumulate in plants. However, the fraction of plant C and N lost in litter fall was decreased in calibrations II and III in which voles are explicitly represented to accommodate the C and N consumed by voles (Table 2:  $m_{CB}$  &  $m_{NB}$  were decreased). Consumption by voles does not increase with plant biomass (Eq. 15), and vole density does not increase with plant biomass because we assume top-down control on voles and therefore use a prescribed vole density. As a consequence, the increase in litter fall as biomass

accumulates is smaller with voles explicitly represented than in the aggregate representation. The accumulation of C and N in vegetation is therefore larger with the explicit inclusion of vole effects than in the simulation where vole effects are aggregated with other processes. When we do allow vole density to increase in proportion of the increase in NPP ( $\sim$ 80% over 100 years), the increase in plant biomass is less than 8% lower because of consumption and the small increase in soil C (<0.5%) becomes a small decrease (<1%).

In addition, because the C:N ratio of forage (19.15 g C g<sup>-1</sup> N) is lower than the C:N ratio of litter (40 g C g<sup>-1</sup> N), the fraction of vegetation N lost in litter fall was decreased more than the fraction of vegetation C lost in litter fall in calibrations II and III with explicit vole representations (Table 2; e.g., 13.7% decrease in litter N versus 6.6% decrease in litter C with 40 vole ha<sup>-1</sup>). As a consequence, as vegetation biomass accumulates, the litter-fall C:N ratio increases more with the explicit representation of voles than with aggregated representation of vole effects. Soil organic C therefore increases more with the explicit vole representation than without it (Fig. 4), and soil organic N decreases more with the explicit vole representation than without it (Fig. 5).

Why is there a synergistic response to elevated CO<sub>2</sub> and warming in combination?

If the response to CO<sub>2</sub> were stronger so that there was a substantial increase in plant biomass and plant C:N ratio, then the feedback associated with litter fall would have come into play and differences between explicit and aggregated representations of vole activity would have made more of a difference by the same mechanism described above for the response to warming.

When elevated CO<sub>2</sub> is combined with warming, the warming mobilizes soil N, easing N limitation of plant production, and the inhibiting feedback on production associated with higher

plant C:N is weakened. This weakening of the C:N feedback allows the direct effects of elevated CO<sub>2</sub> to be more strongly manifested, and hence a stronger response to both elevated CO<sub>2</sub> and warming than the sum of the responses to each factor individually. Tissue and Oechel (1987) found the same synergistic effect resulting in a sustained increase in production with elevated CO<sub>2</sub> and warming but only a transient increase with CO<sub>2</sub> alone.

459

460

461

462

463

464

465

466

467

468

469

470

471

472

473

474

475

476

454

455

456

457

458

#### CONCLUSIONS

Grazing animals can have large effects on ecosystems (Grellman et al., 2002, McLaren and Jefferies 2004, Sjögersten et al., 2008, Post and Pedersen 2008, Rinnan et al., 2009, Cahoon et al., 2011, Kaarlejärvi et et al., 2015, Leffler et al., 2019, Min et al., 2021). Our simulations suggest that long-term exclusion of voles or maintenance of vole populations at high densities can result in large gains or losses of both plants and soil C (Fig. 2). However, the response time of plants and soil to these persistent changes in grazing takes several decades in our model. As a consequence, the full effect of changes in vole densities are never realized when voles cycle on a three-to-four-year time scale. Indeed, cycling at such a high frequency can be incorporated in our model using the long-term mean density without any substantial change in the predicted long-term dynamics of the ecosystem. Our simulations excluding and including voles are not purely academic. Recent studies suggest that arctic rodent population cycles could dampen in amplitude or be punctuated with periods of non-cyclic dynamics in response to altered climate conditions, in particular changes in snow conditions (Gilg 2006, Ims et al., 2008, Kausrud 2008, Brommer et al., 2010, Domine 2018). Our results suggest that the important dynamics for predicting long-term changes in tundra biogeochemistry in response to climate change are the mean grazer dynamics on decadal scales, not the higher frequency three-to-four-year cycles.

The effects of voles on C and N cycling can have major effects on the biogeochemical responses of tundra to elevated CO<sub>2</sub> and warming. These effects need to be explicitly represented in models rather than aggregated with other ecosystem processes. Even if these other processes act in parallel with vole processes, their response to changes in the environment can be very different. Our analysis indicates that failure to explicitly account for voles results in large underestimation of the responses of tundra to climate warming and to elevated CO<sub>2</sub> and warming. Our analysis is analogous to that of Thornton et al., (2007) who found that predicted responses of the terrestrial biosphere to elevated CO<sub>2</sub> and climate change was likely overestimated unless N limitation was explicitly represented in models. We recommend that grazing effects be explicitly incorporated when applying models of tundra response to global change.

Our analysis is based on a simple, annual-time-step model of ecosystem C and N interactions calibrated to arctic tundra. The simplicity of the model facilitates causal tracing (Fig. 7) and heuristic analysis of the results, but at the expense of quantitative detail in the dynamics (Rastetter 2017). The results should therefore be confirmed for more complex models with, for example, more detailed representations of vegetation and soil characteristics, finer-scale seasonal dynamics, and the effects animals can have on plant-community composition and soil structure. Although our model was calibrated for arctic tundra, the qualitative conclusions probably apply more broadly. In our analysis, a key process is vole respiration, which decreases with warming, unlike the increase with warming for plant and microbial respiration. This property is clearly relevant to mammal grazers in cold climates, but not for mammal grazers in warm climates or for insects in any climate. Nevertheless, for these other ecosystems there might be analogous model biases associated with aggregating biogeochemical processes

mediated by these grazers with other ecosystem processes. Similarly, the consequences of resource limitation need to be examined for grazers in ecosystems that are bottom-up regulated. All these possibilities need to be analyzed, first with heuristic models like the one we use and then incorporated into more detailed biogeochemical models. To perform these analyses, more data like those in Batzli et al. (1980) and Olofsson et al. (2012) are needed that can be directly applied in these biogeochemical models. Collection of these data will require a biogeochemical, as well as a community, perspective on plant-grazer interactions.

# **ACKNOWLEDGEMENTS**

This work was supported in part by the National Science Foundation under NSF grants 1651722, 1637459, 1603560, 1556772, 1841608 to E.B.R.; 1603777 to N.T.B. and K.L.G.; 1603654 to R.J.R.; 1603760 to L.G.; 1603677 to J.R.M. Any opinions, findings and conclusions or recommendations expressed in this material are those of the authors and do not necessarily reflect those of the National Science Foundation. We also want to thank Bonnie Kwiatkowski for assistance with code development and archiving.

# LITERATURE CITED

517

518 Batzli, G. O., R. G. White, S. F. MacLean Jr, F. A. Pitelka, and B. D. Collier. 1980. The 519 herbivore-based trophic system. pp 335-410 in Brown, J., Miller, P.C., Tieszen, L.L., and 520 Brunnell, F.L. eds.. An Arctic Ecosystem: the Coastal Tundra at Barrow, Alaska. 521 Dowden, Hutchinson, and Ross Inc, Stroudsburg, PA, USA 522 Bennett, V. J. 2003. Computer modelling the Serengeti-mara ecosystem. Doctor of Philosophy 523 dissertation, School of Biology, The University of Leeds. 524 Brommer, J. E., H. Pietianen, K. Ahola, P. Karell, T. Karstinen, and H. Kolunen. 2010. The 525 return of the vole cycle in southern Finland refutes generality of the loss of cycles 526 through 'climatic forcing'. Global Chance Biology 16:577-586 527 Cahoon, S. M. P., P. F. Sullivan, E. Post, and J. M. Welker. 2011. Large herbivores limit CO2 528 uptake and suppress carbon cycle responses to warming in West Greenland. Global 529 Change Biology 18:469–479. 530 Carey, J. C., J. Tang, P. H. Templar, K. D. Kroger, T. W. Crowther, A. J. Burton, J. S. Dukes, B. 531 Emmett, S. D. Frey, M. A. Heskel, L. Jiang, M. B. Machmuller, J. Mohan, A. M. 532 Panetta, P. B. Reich, S. Reinsch, X. Wang, S. D. Allison, C. Bamminger, S. Bridgham, S. 533 L. Collins, G. de Dato, W. C. Eddy, B. J. Enquist, M. Estiarte, J. Harte, A. Henderson, B. 534 R. Johnson, K. S. Larsen, Y. Luo, S. Marhan, J. M. Melillo, J. Peñuelas, L. Pfeifer-535 Meister, C. Poll, E. Rastetter, A. B. Reinmann, L. L. Reynolds, I. K. Schmidt, G. R. 536 Shaver, A. L. Strong, V. Suseela, and A. Tietema. 2016. Temperature response of soil 537 respiration largely unaltered with experimental warming. Proc Nat Accad Sci 113:13797-538 13802.

539	Domine, F., Gauthier G., Vionnet V., Fauteux D., Dumont M., and Barrere M. 2018. Snow
540	physical properties may be a significant determinant of lemming population dynamics in
541	the high Arctic, Arctic Science, 4: 813–826 <a href="https://doi.org/10.1139/as-2018-0008">https://doi.org/10.1139/as-2018-0008</a>
542	Ehrich, D., N.M. Schmidt, G. Gauthier, R. Alisauskas, A. Angerbjörn, K. Clark, F. Ecke, N.E.
543	Eide, E. Framstad, J. Frandsen, A. Franke, O. Gilg, M.A. Giroux, H. Henttonen, B.
544	Hörnfeldt, R.A. Ims, G.D. Kataev, S.P. Kharitonov, S.T. Killengreen, C.J. Krebs, R.B.
545	Lanctot, N. Lecomte, I.E. Menyushina, D.W. Morris, G. Morrisson, L. Oksanen, T.
546	Oksanen, J. Olofsson, I.G. Pokrovsky, I.Y. Popov, D. Reid, J.D. Roth, S.T. Saalfeld, G.
547	Samelius, B. Sittler, S.M. Sleptsov, P.A. Smith, A.A. Sokolov, N.A. Sokolova, M.Y.
548	Soloviev, D.V. Solovyeva. 2020. Documenting lemming population change in the Arctic
549	Can we detect trends? Ambio 49:786-800. doi: 10.1007/s13280-019-01198-7.
550	Gilg, O., B. Sittler, and I. Hanski. 2009. Climate change and cyclic predator-prey population
551	dynamics in the high Arctic. Glob. Change Biol. 15, 2634-265210.1111/j.1365-
552	2486.2009.01927.x doi:10.1111/j.1365-2486.2009.01927.x.
553	Gough, L., J. C. Moore, G. R. Shaver, R. T. Simpson, and D. R. Johnson. 2012. Above- and
554	belowground responses of arctic tundra to altered soil nutrients and mammalian
555	herbivory. Ecology 93:1683-1694.
556	Grellman, D. 2002. Plant responses to fertilization and exclusion of grazers on an arctic tundra
557	heath. Oikos, 98:190–204.
558	Hairston, N. G., F. E. Smith, and L. B. Slobodkin. 1960. Community structure, population
559	control, and competition. The American Naturalist 94:421-425.
560	Heskel, M. A., O. S. O'Sullivan, P. B. Reich, M. G. Tjoelker, L. K. Weerasinghe, A. Penillard, J.
561	J. G. Egerton, D. Creek, K. J. Bloomfield, J. Xiang, F. Sinca, Z. R. Stangl, A. Martinez-

562	de la Torre, K. L. Greffin, C. Huntingford, V. Hurry, P. Meir, M. H. Turnbull, and O. K.		
563	Atkin. 2016. Convergence in the temperature response of leaf respiration across biomes		
564	and plant functional types. Proc Nat Accad Sci 113: 3832-3837.		
565	Ims, R. A., J. A. Henden, and S. T. Killengreen. 2008. Collapsing population cycles. Trends		
566	Ecol. Evol. 23, 79–8610.1016/j.tree.2007.10.010 doi:10.1016/j.tree.2007.10.010.		
567	Jai, S., X. Wang, Z. Yuan, F. Lin, Z. Hao, and M.S. Luskin. 2018. Global signal of top-down		
568	control of terrestrial plant communities by herbivores. Proceedings of the National		
569	Academy of Sciences 115, 6237-6242. DOI: 10.1073/pnas.1707984115.		
570	Jiang, Y., E. B. Rastetter, G. R. Shaver, A. V. Rocha, Q. Zhuang, and B. L. Kwiatkowsk. 2017.		
571	Modeling long-term changes in tundra carbon balance following wildfire, climate change		
572	and potential nutrient addition. Ecological Applications 27:105-117		
573	Kaarlejärvi, E., K. S. Hoset, and J. Olofsson. 2015. Mammalian herbivores confer resilience of		
574	arctic shrub-dominated ecosystems to changing climate. Global Change Biology 21,		
575	3379-3388.		
576	Kausrud, K. L., A. Mysterud, H. Steen, J. O. Vik, E. Ostbye, B. Cazelles, E. Framstad, A. M.		
577	Eikeset, I. Mysterud, T. Solhoy, and N. C. Stenseth. 2008. Linking climate change to		
578	lemming cycles. Nature 456, 93-9710.1038/nature07442 doi:10.1038/nature07442.		
579	Korpimaki, E., P. R. Brown, J. Jacobs, and R. P. Pech. 2004. The puzzles of population cycles		
580	and outbreaks of small mammals solved? Bioscience 5412.:1071-1079		
581	Krebs, C. J. 2013. Population fluctuations in rodents. University of Chicago Press, Chicago, IL		
582	USA		

583 Krebs, C. J., R. Boonstra, and A. J. Kenney. 1995. Population dynamics of the collared lemming 584 and the tundra vole at Pearce Point, Northwest Territories, Canada. Oecologia 103:481-585 489. 586 Leffler, A. J., K. H. Beard, K. C. Kelsey, R. T. Choi, J. A. Schmutz, and J. M. Welker. 2019. 587 Delayed herbivory by migratory geese increases summer-long CO2 uptake in coastal 588 western Alaska. Global Change Biology, 25, 277–289. 589 Legagneux, P., G. Gauthier, D. Berteaux, J. Bêty, M. C. Cadieux, F. Bilodeau, E. Bolduc, L. 590 McKinnon, A. Tarroux, J. F. Therrien, L. Morissette, and C. J. Krebs. 2012. 591 Disentangling trophic relationships in a high arctic tundra ecosystem through food web 592 modeling. Ecology 93:1707-1716 593 McGuire, A. D., T. R. Christensen, D. Hayes, A. Heroult, E. Euskirchen, J. S. Kimball, C. 594 Koven, P. Lafleur, P. A. Miller, W. Oechel, P. Peylin, M. Williams, and Y. Yi. 2012. An 595 assessment of the carbon balance of arctic tundra: Comparisons among observations, 596 process models, and atmospheric inversions. Biogeosciences 9:3185-3204. 597 McKane, R., E. Rastetter, G. Shaver, K. Nadelhoffer, A. Giblin, J. Laundre, and F. Chapin. 1997. 598 Reconstruction and analysis of historical changes in carbon storage in arctic tundra. 599 Ecology 78:1188-1198. 600 McKinnon, L., P. A. Smith, E. Nol, J. L. Martin, F. I. Doyle, F.I., Abraham, H. G. Gilchrist, R. I. 601 G. Morrison, and J. Bêty. 2010. Lower predation risk for migratory birds at high 602 latitudes. Science 327:326-327 603 McLaren, J. R., and R. L. Jefferies. 2004.. Initiation and maintenance of vegetation mosaics in an 604 Arctic salt marsh. J Ecol 92:648-660.

605 McNaughton, S. J. 1985. Ecology of a grazing ecosystem: The Serengeti. Ecological 606 Monographs 55:259-294. 607 Metcalfe, D. B., G. P. Asner, R. E. Martin, J. E. Silva Espejo, W. H. Huasco, F. F. Farfán 608 Amézquita, L. Carranza-Jimenez, D. F. Galiano Cabrera, L.D. Baca, F. Sinca, L. P. 609 Huaraca Quispe, I. A. Taype, L. E. Mora, A. R. Dávila, M. M. Solórzano, B. L. Puma 610 Vilca, J. M. Laupa Román, P. C. Guerra Bustios, N. S. Revilla, R. Tupayachi, C. J. 611 Girardin, C. E. Doughty, and Y. Malhi. 2014. Herbivory makes major contributions to 612 ecosystem carbon and nutrient cycling in tropical forests. Ecology Letters 17:324–32. 613 doi: 10.1111/ele.12233 614 Metclafe, D. B., and J. Olofsson. 2015. Distinct impacts of different mammalian herbivore 615 assemblages on arctic tundra CO2 exchange during the peak of the growing season. 616 Oikos 124: 1632-1638. https://doi.org/10.1111/oik.02085 617 Min, E., M. Wilcots, S. Naeem, L. Gough, J. R. McLaren, R. J. Rowe, E. Rastetter, N. Boelman, 618 and K. L. Griffin. 2021. Herbivore absence can shift dry heath tundra from carbon source 619 to sink during peak growing season. Environ. Res. Lett. 162021. 024027 620 Oli, M. 2019. Population cycles in voles and lemmings: state of the science and future directions. 621 Mammal Review 49 2019. 226–239Roberts, P and Jones DL. 2012. Microbial and plant 622 uptake of free amino sugars in grassland soils. Soil Biology and Biochemistry 49:139-149. 623 624 Olofsson, J., H. Tømmervik, and T. V. Callaghan. 2012. Vole and lemming activity observed 625 from space. Nature Climate Change Letters DOI: 10.1038/NCLIMATE1537 626 Pastor, J. R., J. Naiman, B. Dewey. and P. McInnes. 1988. Moose, microbes and the boreal 627 forest. Bioscience 38:770-779.

628 Pearce, A. R., E. B. Rastetter, W. B. Bowden, M. C. Mack, Y. Jiang, Y., and B. L. Kwiatkowski, 629 B.L. 2015. Recovery of arctic tundra from thermal erosion disturbance is constrained by 630 nutrient accumulation: a modeling analysis. Ecological Applications 25:1271-1289. 631 Petit Bon, M., K. G. Inga, I. S. Jónsdóttir, T. A. Utsi, E. M. Soininen, and K. A. Bråthen. 2020. 632 Interactions between winter and summer herbivory affect spatial and temporal plant 633 nutrient dynamics in tundra grassland communities. Oikos 129:1229-1242. 634 Pitelka, F. A. and G. O. Batzli. 2007. Population cycles of lemmings near Barrow, Alaska: a 635 historical review. Acta Theriologica 52: 323–336. 636 Pitelka, F. A., P. Q. Tomich, and G. W. Treichel. 1955. Ecological relations of jaegers and owls 637 as lemming predators near Barrow, Alaska. Ecological Monographs 25: 85–117. 638 Post, E., and C. Pedersen. 2008. Opposing plant community responses to warming with and 639 without herbivores. Proceedings of the National Academy of Sciences 105, 12353-12358. 640 Prevedello, J. M., C. R. Dickman, M. V. Vieira, and E. M. Vieira, E.M. 2013. Population 641 responses of small mammals to food supply and predators: a global meta-analysis. J 642 Animal Ecol. 82:927-936. 643 Rastetter, EB. 2017. Modeling for understanding v. modeling for numbers. Ecosystems 20:215-644 221. 645 Rastetter, E. B., G. I. Ågren, and G. R. Shaver. 1997. Responses of N-limited ecosystems to 646 increased CO2: A balanced-nutrition, coupled-element-cycles model. Ecol. Appl. 7: 444— 647 460. 648 Rastetter, E., K. Griffin, R. Rowe, L. Gough, J. McLaren, and N. Boelman. 2021a. ARC-LTER/vole: 649 Initial release - VOLE v4.0 (Version v4.0). Zenodo. http://doi.org/10.5281/zenodo.5083290 650 Rastetter, E., K. Griffin, R. Rowe, L. Gough, J. McLaren, and N. Boelman. 2021b. Modeling the effect of 651 explicit vs implicit representation of grazing on ecosystem carbon and nitrogen cycling in

652	response to elevated carbon dioxide and warming in arctic tussock tundra, Alaska - Dataset A ver
653	2. Environmental Data Initiative.
654	https://doi.org/10.6073/pasta/67108cef344d93cfdd060e7e0f0911f5.
655	Rastetter, E., K. Griffin, R. Rowe, L. Gough, J. McLaren, and N. Boelman. 2021c. Modeling the effect of
656	explicit vs implicit representation of grazing on ecosystem carbon and nitrogen cycling in
657	response to elevated carbon dioxide and warming in arctic tussock tundra, Alaska - Dataset B ver
658	2. Environmental Data Initiative.
659	$\underline{https://doi.org/10.6073/pasta/42e6660b2d1f2b59985ed0940e53f0d4}.$
660	Rastetter, E. B., G. W. Kling, G. R. Shaver, B. C. Crump, L. Gough, and K. L. Griffin. 2020.
661	Ecosystem recovery from disturbance is constrained by N cycle openness, vegetation-soil
662	N distribution, form of N losses, and the balance between vegetation and soil-microbial
663	processes. Ecosystems https://doi.org/10.1007/s10021-020-00542-3
664	Rinnan, R., S. Stark, and A. Tolvanen. 2009. Responses of vegetation and soil microbial
665	communities to warming and simulated herbivory in a subarctic heath. Journal of
666	Ecology 97:788–800.
667	Schmitz, O. J., P. A. Raymond, J. A. Estes, W. A. Kurz, G. W. Holtgrieve, M. E. Ritchie, D. E.
668	Schindler, A. C., Spivak, R. W. Wilson, M. A. Bradford, V. Christensen, L. Deegan, V.
669	Smetacek, M. J. Vanni, and C. C. Wilmers. 2014. Animating the carbon cycle.
670	Ecosystems 17:344-359.
671	Seagle, S. W. and S. J. McNaughton. 1993. Simulated effects of precipitation and nitrogen on
672	Serengeti grassland productivity. Biogeochemistry, 22,157-178.
673	Sjögersten, S., R. van der Wal, and S. J. Woodin. 2008 Habitat type determines herbivory
674	controls over CO2 fluxes in a warmer Arctic. Ecology 89:2103–16.

675	Thornton, P. E., J. F. Lamarque, N. A. Rosenbloom, and N. M. Mahowald. 2007. Influence of
676	carbon-nitrogen cycle coupling on land model response to CO2 fertilization and climate
677	variability. Global Biogeochemical Cycles 21 GB4018, doi:10.1029/2006GB002868
678	Tissue, D. T., and W. C. Oechell. 1987. Response of Eriophorum vaginatum to elevated CO2
679	and temperature in the Alaskan tussock tundra. Ecology 68:401-410.
680	Tuomi, M., S. Stark, K. S. Hoset, M. Väisänen, L. Oksanen, F. J. A. Murguzur, H. Tuomisto, J.
681	Dahlgren, and K. A. Bråthen, K.A. 2019. Herbivore effects on ecosystem process rates in
682	a low-productive system. Ecosystems 22:827-843.
683	Wardle, D. A., R. D. Bardgett, J. N. Klironomos, H. Setälä, W. H., Van der Putten, and D. H.
684	Wall. 2004. Ecological linkages between aboveground and belowground biota. Science
685	304:1629-1633
686	Wilkinson, D. M., and T. N. Sherratt. 2016. Why is the world green? The interactions of top-
687	down and bottom-up processes in terrestrial vegetation ecology, Plant Ecology and
688	Diversity, 9:2, 127-140, DOI: 10.1080/17550874.2016.1178353
689	Yu, Q., H. E. Epstein, D. A. Walker, G. V. Frost, and B. C. Forbes. 2011. Modeling dynamics of
690	tundra plant communities on the Yamal Peninsula, Russia, in response to climate change
691	and grazing pressure. Environmental Research Letters 6. doi:10.1088/1748-
692	9326/6/4/045505.
693	Zimov, N. S., S. A. Zimov, A. E. Zimova, G. H. Zimova, V. I. Chuprynin, and F. S. Chapin III.
694	2009. Carbon storage in permafrost and soils of the mammoth tundra-steppe biome: Role
695	in the global carbon budget. Geophysical Research Letters 36.
696	doi:10.1029/2008GL036332.

**Box 1:** Model Equations. Variables and parameters defined in Table 1.

	MASS-BALANCE EQUATIONS				
1	$\frac{dB_{\rm C}}{dt} = P_{\rm s} - L_{\rm itC} - R_a - G_{\rm C}$	2	$\frac{dB_{\rm N}}{dt} = U_{\rm N} - L_{\rm itN} - G_{\rm N}$		
3	$\frac{dD_{C}}{dt} = L_{itC} + L_{VC} - R_{h} - Q_{CR}$	4	$\frac{dD_{N}}{dt} = L_{itN} + U_{Nm} + L_{VN}$ $-N_{min} - Q_{NR}$		
		5	$\frac{dN}{dt} = N_{\text{in}} + N_{\text{min}} + V_{\text{UN}} - U_{\text{N}}$ $- U_{\text{Nm}} - Q_{\text{DIN}}$		
	ALLOMETRY & STOICH	ION	METRY CONSTRAINTS		
6	$S = B_{C} \frac{\left( \propto B_{C} + 1 \right)}{\left( \gamma B_{C} + 1 \right)}$				
7	$\Psi = \frac{B_{\rm C}}{B_{\rm N} q_{\rm B}}$	8	$\Phi = \frac{D_{\mathrm{C}}}{D_{\mathrm{N}} q_{\mathrm{D}}}$		
	PROCESS	EQU	ATIONS		
	CARBON		NITROGEN		
9	$P_{s} = \frac{g_{C} S C_{a}}{\Psi(k_{C} + C_{a})} Q_{10Ps}^{T/10}$	10	$U_{\rm N} = \frac{g_{\rm N} \Psi \ S N}{k_{\rm N} + N} Q_{10{\rm U}}^{T/10}$		
11	$L_{\text{itC}} = m_{\text{CB}} B_{\text{C}}$	12	$L_{\text{itN}} = \frac{m_{\text{NB}}}{\Psi} B_{\text{N}}$		

13	$R_{\rm a} = r_{\rm B} B_{\rm C} \Psi Q_{\rm 10Ra}^{T/10}$	14	$U_{\rm Nm} = \frac{g_{\rm Nm} \Phi D_{\rm C} N}{k_{\rm Nm} + N} Q_{10{\rm Um}}^{T/10}$
15	$G_C = \left(n_V + g_V - \varepsilon_V \left(T - T_0\right)\right) V / 10000$	16	$G_{\rm N} = G_{\rm C}/q_{\rm V}$
17	$R_{\mathrm{V}} = r_{\mathrm{V}} \left( G_{\mathrm{C}} - n_{\mathrm{V}} V / 10000 \right)$	18	$V_{\rm UN} = m_{\rm NV} V / 10000$
19	$L_{\rm VC} = G_{\rm C} - R_{\rm V}$	20	$L_{\rm VN} = G_{\rm N} - V_{\rm UN}$
21	$R_{\rm h} = r_{\rm D} D_{\rm C} \Phi Q_{\rm 10Rh}^{T/10}$	22	$N_{\min} = \frac{m_{\text{Nm}} D_{\text{N}}}{\Phi} Q_{10\text{m}}^{T/10}$
23	$Q_{\rm CR} = q_{\rm DOM} Q_{\rm NR}$	24	$Q_{\rm NR} = \beta_{\rm NR} D_{\rm N}$
		25	$Q_{\rm DIN} = \beta_{\rm N} N$

**Table 1:** Model variables and parameters. Variable values are for the initial steady state with the aggregated representation of vole effects.  $\Psi$  and  $\Phi$  are assumed to equal 1 under this steady state.  $Q_{10}$  values are as reported in the main text. Other values are from Pearce et al. (2015) or are fit to analogous functions in Pearce et al. (2015). Parameters are listed to four significant digits.

	Symbol	Value	Units
C and N stocks			
Vegetation C	B <sub>C</sub>	878	g C m <sup>-2</sup>
Detritus and soil organic C	$D_{\mathrm{C}}$	19452	g C m <sup>-2</sup>
Vegetation N	$B_{ m N}$	20.6	g N m <sup>-2</sup>
Detritus and soil organic N	$D_{ m N}$	831	g N m <sup>-2</sup>
Inorganic N	N	0.27	g N m <sup>-2</sup>
Processes and constraints			
Allometric constraint	S	243.75	g C m <sup>-2</sup>
Vegetation stoichiometric constraint	Ψ	1	none
Soil stoichiometric constraint	Φ	1	none
Photosynthesis	$P_{\rm s}$	430	g C m <sup>-2</sup> yr <sup>-1</sup>
Autotrophic respiration	Ra	215	g C m <sup>-2</sup> yr <sup>-1</sup>
Litter-fall C	$L_{ m itC}$	215	g C m <sup>-2</sup> yr <sup>-1</sup>
Heterotrophic respiration (excluding voles)	$R_{ m h}$	213.07	g C m <sup>-2</sup> yr <sup>-1</sup>
Vegetation N uptake	$U_{ m N}$	5.3800	g N m <sup>-2</sup> yr <sup>-1</sup>
Litter-fall N	$L_{ m itN}$	5.3800	g N m <sup>-2</sup> yr <sup>-1</sup>
Gross N mineralization	$N_{ m min}$	19.7310	g N m <sup>-2</sup> yr <sup>-1</sup>
N immobilization	$U_{ m Nm}$	14.4824	g N m <sup>-2</sup> yr <sup>-1</sup>
Inorganic N losses	$Q_{\mathrm{DIN}}$	0.0016	g N m <sup>-2</sup> yr <sup>-1</sup>

Refractory N losses	$Q_{ m NR}$	0.1314	g N m <sup>-2</sup> yr <sup>-1</sup>
Refractory C losses	$Q_{\mathrm{CR}}$	1.93	g C m <sup>-2</sup> yr <sup>-1</sup>
C removed from vegetation by voles	$G_{\mathrm{C}}$	0	g C m <sup>-2</sup> yr <sup>-1</sup>
Vole respiration	$R_{ m V}$	0	g C m <sup>-2</sup> yr <sup>-1</sup>
C added to soil organic matter by voles	$L_{ m VC}$	0	g C m <sup>-2</sup> yr <sup>-1</sup>
N removed from vegetation by voles	$G_{ m N}$	0	g N m <sup>-2</sup> yr <sup>-1</sup>
C added to soil organic matter by voles	$L_{ m VN}$	0	g N m <sup>-2</sup> yr <sup>-1</sup>
Vole N transfer vegetation to inorganic soil	$V_{ m UN}$	0	g N m <sup>-2</sup> yr <sup>-1</sup>
Driver variables			
Atmospheric CO2	$C_{\mathrm{a}}$	400	μmol mol <sup>-1</sup>
Temperature	T	10	°C
N inputs	$N_{ m in}$	0.1330	g N m <sup>-2</sup> yr <sup>-1</sup>
Voles	V	0	voles ha <sup>-1</sup>
Parameters			
Allometric parameter 1	α	0.002231	m² g-1 C
Allometric parameter 2	γ	0.01100	m² g <sup>-1</sup> C
Optimum vegetation C:N	$q_{ m B}$	42.62	g C g <sup>-1</sup> N
Optimum soil C:N	$q_{ m D}$	23.41	g C g <sup>-1</sup> N
Photosynthesis rate parameter	<b>g</b> c	1.423	yr <sup>-1</sup>
CO <sub>2</sub> half-saturation constant	$k_{\mathrm{C}}$	100.0	μmol mol <sup>-1</sup>
Photosynthesis Q-10	$Q_{ m 10Ps}$	1.550	none
Autotrophic respiration constant	$r_{ m B}$	0.09069	yr <sup>-1</sup>
Autotrophic respiration Q-10	$Q_{ m 10Ra}$	2.700	none
Vegetation C turnover rate constant	<i>т</i> СВ	0.2449	yr <sup>-1</sup>

Vegetation N-uptake rate parameter	$g_{ m N}$	0.05191	g N g <sup>-1</sup> C yr <sup>-1</sup>
Vegetation N half-saturation constant	$k_{ m N}$	1.000	g N m <sup>-2</sup>
Vegetation N-uptake Q-10	$Q_{ m 10U}$	2.000	none
Vegetation N turnover rate constant	$m_{ m NB}$	0.2612	yr <sup>-1</sup>
Heterotrophic respiration constant	$r_{ m D}$	0.003651	yr <sup>-1</sup>
Heterotrophic respiration Q-10	$Q_{ m 10Rh}$	3.000	none
Microbial N-uptake rate parameter	$g_{ m Nm}$	0.001796	g N g <sup>-1</sup> C yr <sup>-1</sup>
Microbial N half-saturation constant	$k_{ m Nm}$	1.000	g N m <sup>-2</sup>
Microbial N-uptake Q-10	$Q_{ m 10Um}$	1.950	none
Vole nesting material	$n_{ m V}$	22	g C vole <sup>-1</sup> yr <sup>-1</sup>
Vole C ingestion rate	gv	3512	g C vole <sup>-1</sup> yr <sup>-1</sup>
Temperature slope vole metabolism	εν	52	g C vole <sup>-1</sup> °C <sup>-1</sup> yr <sup>-1</sup>
Summer to annual temperature correction	$T_0$	10	°C
C:N of vole forage and nest material	$q_{ m V}$	19.15	g C g <sup>-1</sup> N
Vole base respiration rate	ľV	0.3	none
Vole urine N production rate	$m_{ m NV}$	11.00	g N vole <sup>-1</sup> yr <sup>-1</sup>
Soil organic N turnover constant	$m_{ m Nm}$	0.01099	yr <sup>-1</sup>
Soil organic N turnover Q-10	$Q_{ m 10m}$	2.160	none
C:N of DOM loss	q <sub>DOM</sub>	14.69	g C g <sup>-1</sup> N
N loss-rate parameter	$\beta_{ m N}$	0.005926	yr <sup>-1</sup>
Refractory N loss parameter	$\beta_{ m NR}$	0.0001581	yr <sup>-1</sup>

**Table 2:** Variable and parameter changes to accommodate the effect of explicit representation of voles. Values in parentheses are the percent change from the values used in the implicit-vole representation with vole effects aggregated in with parallel ecosystem processes. "Total" is the total of the vole-mediated and the parallel ecosystem process in the two preceding rows. "PAR" is the parameter in the equation for the parallel process in the preceding rows that was modified to accommodate explicit representation of voles.

		vole effects aggregated in with other	explicit vole representation with	explicit vole representation	
	Symbol	processes	40 voles ha <sup>-1</sup>	with 100 voles ha <sup>-1</sup>	units
	$L_{ m itC}$	215	200.864 (-6.6%)	179.66 (-16.4%)	g C m <sup>-2</sup> yr <sup>-1</sup>
	$G_{\mathrm{C}}$	0	14.136	35.34	g C m <sup>-2</sup> yr <sup>-1</sup>
Total		215	215	215	g C m <sup>-2</sup> yr <sup>-1</sup>
PAR	m <sub>CB</sub>	0.2449	0.2288 (-6.6%)	0.2046 (-16.4%)	yr <sup>-1</sup>
	$R_{ m h}$	213.07	208.8556 (-2.0%)	202.534 (-4.9%)	g C m <sup>-2</sup> yr <sup>-1</sup>
	$R_{ m v}$	0	4.2144	10.536	g C m <sup>-2</sup> yr <sup>-1</sup>
Total		213.07	213.07	213.07	g C m <sup>-2</sup> yr <sup>-1</sup>
PAR	r <sub>D</sub>	0.003651	0.003658 (-2.0%)	0.003471 (-4.9%)	yr <sup>-1</sup>
	$L_{ m itN}$	5.38	4.6418 (-13.7%)	3.5346 (-34.3%)	g N m <sup>-2</sup> yr <sup>-1</sup>

	$G_{ m N}$	0	0.7382	1.8454	g N m <sup>-2</sup> yr <sup>-1</sup>
Total		5.38	5.38	5.38	g N m <sup>-2</sup> yr <sup>-1</sup>
PAR	$m_{ m NB}$	0.2612	0.2253 (-13.7%)	0.1716 (-34.3%)	yr <sup>-1</sup>
	$V_{ m UN}$	0	0.044	0.110	g N m <sup>-2</sup> yr <sup>-1</sup>
	$N_{ m min}$	19.731	19.687 (-0.2%)	19.621 (-0.6%)	g N m <sup>-2</sup> yr <sup>-1</sup>
Total		19.731	19.731	19.731	g N m <sup>-2</sup> yr <sup>-1</sup>
PAR	$m_{ m Nm}$	0.01099	0.01097 (-0.2%)	0.01093 (-0.6%)	yr <sup>-1</sup>

# **Table 3:** Calibrations

Calibration	Vole representation	Vole density
I	vole effects aggregated in	Unspecified vole density, but vole effects
	with other processes	subsumed into litter fall C and N, heterotrophic
		respiration, and N mineralization in the calibration
		(Table 2).
II	explicit vole	40 voles ha <sup>-1</sup>
	representation	
III	explicit vole	100 voles ha <sup>-1</sup>
	representation	

# **Table 4**: Simulations

Simu-	Cali-	Description	Figure
lation	bration		
Set 1:			
1	II	constant 40 voles ha <sup>-1</sup>	Fig. 2 dotted black
			lines
2	II	voles cycling as in Fig. 1	Fig. 2 cycling black
			solid lines
3	II	voles cycling as in Fig. 1 for 10 years then held	Fig. 2 dashed red
		constant at 100 voles ha <sup>-1</sup>	lines
4	II	voles cycling as in Fig. 1 for 10 years then held	Fig. 2 dash-dotted
		constant at 0 voles ha <sup>-1</sup>	blue lines
Set 2:			
5	Ι	vole density unspecified, linear increase of CO <sub>2</sub>	Figs. 4, 5, & 6 dotted
		from 400 to 800 μmol mol <sup>-1</sup> over 100 years	line, left column
6	Ι	vole density unspecified, linear increase in	Figs. 4, 5, & 6 dotted
		temperature from 10 to 15 °C over 100 years	line, middle column
7	I	vole density unspecified, linear increase of CO <sub>2</sub>	Figs. 4, 5, & 6 dotted
		from 400 to 800 µmol mol <sup>-1</sup> and temperature from	line, right column
		10 to 15 °C over 100 years	
8	II	vole density cycling as in Fig. 1, linear increase of	Figs. 4, 5, & 6 blue
		CO <sub>2</sub> from 400 to 800 µmol mol <sup>-1</sup> over 100 years	solid line, left
			column

9	II	vole density cycling as in Fig. 1, linear increase in	Figs. 4, 5, & 6 blue	
		temperature from 10 to 15 °C over 100 years	solid line, middle	
			column	
10	II	vole density cycling as in Fig. 1, linear increase of Figs. 4, 5, & 6 blue		
		CO <sub>2</sub> from 400 to 800 µmol mol <sup>-1</sup> and temperature	solid line, right	
		from 10 to 15 °C over 100 years	column	
11	III	constant 100 voles ha <sup>-1</sup> , linear increase of CO <sub>2</sub> from	Figs. 4, 5, & 6	
		400 to 800 μmol mol <sup>-1</sup> over 100 years	dashed red line, left	
			column	
12	III	constant 100 voles ha <sup>-1</sup> , linear increase in	Figs. 4, 5, & 6	
		temperature from 10 to 15 °C over 100 years	dashed red line,	
			middle column	
13	III	constant 100 voles ha <sup>-1</sup> , linear increase of CO <sub>2</sub> from	Figs. 4, 5, & 6	
		400 to 800 μmol mol <sup>-1</sup> and temperature from 10 to	dashed red line, right	
		15 °C over 100 years	column	

#### FIGURE CAPTIONS

**Figure 1:** Vole cycle used to simulate ecosystem response to grazing. Vole abundance is randomly generated with peaks every three or four years, with abundances at the peak ranging from 90 to 110 voles ha<sup>-1</sup>, minimum abundances ranging from 8 to 12 voles ha<sup>-1</sup>, and a mean vole abundance of 40 voles ha<sup>-1</sup>. Upper panel shows the first 30 years of the time series. Bottom panel is the full 200-year time series.

**Figure 2:** Simulated changes in plant and soil organic carbon (C) and nitrogen (N) in response to constant vole abundance, vole cycling, vole density maintained at 100 voles ha<sup>-1</sup>, and vole removal (see Table 4). The thin dotted black lines are the steady state values if vole density is held at 40 voles ha<sup>-1</sup> (simulation 1). Solid black lines are the responses to the vole cycle depicted in figure 1 (simulation 2). Dashed red lines are the responses to the same vole cycle and then vole density maintained at 100 voles ha<sup>-1</sup> after year 10 (simulation 3). Dashed-dotted blue lines are the responses to the same vole cycle and then removal of voles after year 10 (simulation 4).

**Figure 3:** Plant carbon (C) and nitrogen (N) recovery following peak vole abundance in simulation 2. The plant C and N of 875 g C m<sup>-2</sup> and 20.2 g N m<sup>-2</sup> were selected to partition the recovery time series into two approximately equal-sized groups based on their values at the time of the previous vole peak (time 0 on x axis). The levels of C and N during this recovery depend not only on peak vole abundance, but also on the degree of recovery following the previous vole cycle. Because the biomass consumed is proportional to vole abundance and not to plant biomass, if plants recover to a higher level following the previous cycle (white dots), then they

begin and maintain recovery in the current cycle at a higher level relative to plants that recovered to a lower level in the previous cycle (black dots). This autocorrelation results in the longer-term dynamics in Fig. 2 for simulation 2 in which vole abundance cycled. The recovery in any cycle also depends on vole abundance and the duration of the vole cycle (higher plant recovery in a 4year cycle than a 3-year cycle).

750

751

752

753

754

755

756

757

745

746

747

748

749

Figure 4: Simulated changes in plant, soil, and total ecosystem C with a linear increase in CO<sub>2</sub> from 400 to 800 µmol mol<sup>-1</sup> over 100 years, a linear warming from 10 to 15 °C over 100 years, and both a linear increase in CO<sub>2</sub> from 400 to 800 µmol mol<sup>-1</sup> and a linear warming from 10 to 15 °C over 100 years (see Table 4). Different trajectories indicate responses with vole effects aggregated with other biogeochemical processes (dotted black lines; simulations 5, 6, & 7), voles cycling between 8 and 110 voles ha<sup>-1</sup> on a three-to-four-year cycle (solid blue lines; simulations 8, 9, & 10), and a constant 100 voles ha<sup>-1</sup> (dashed red lines; simulations 11, 12, & 13).

758

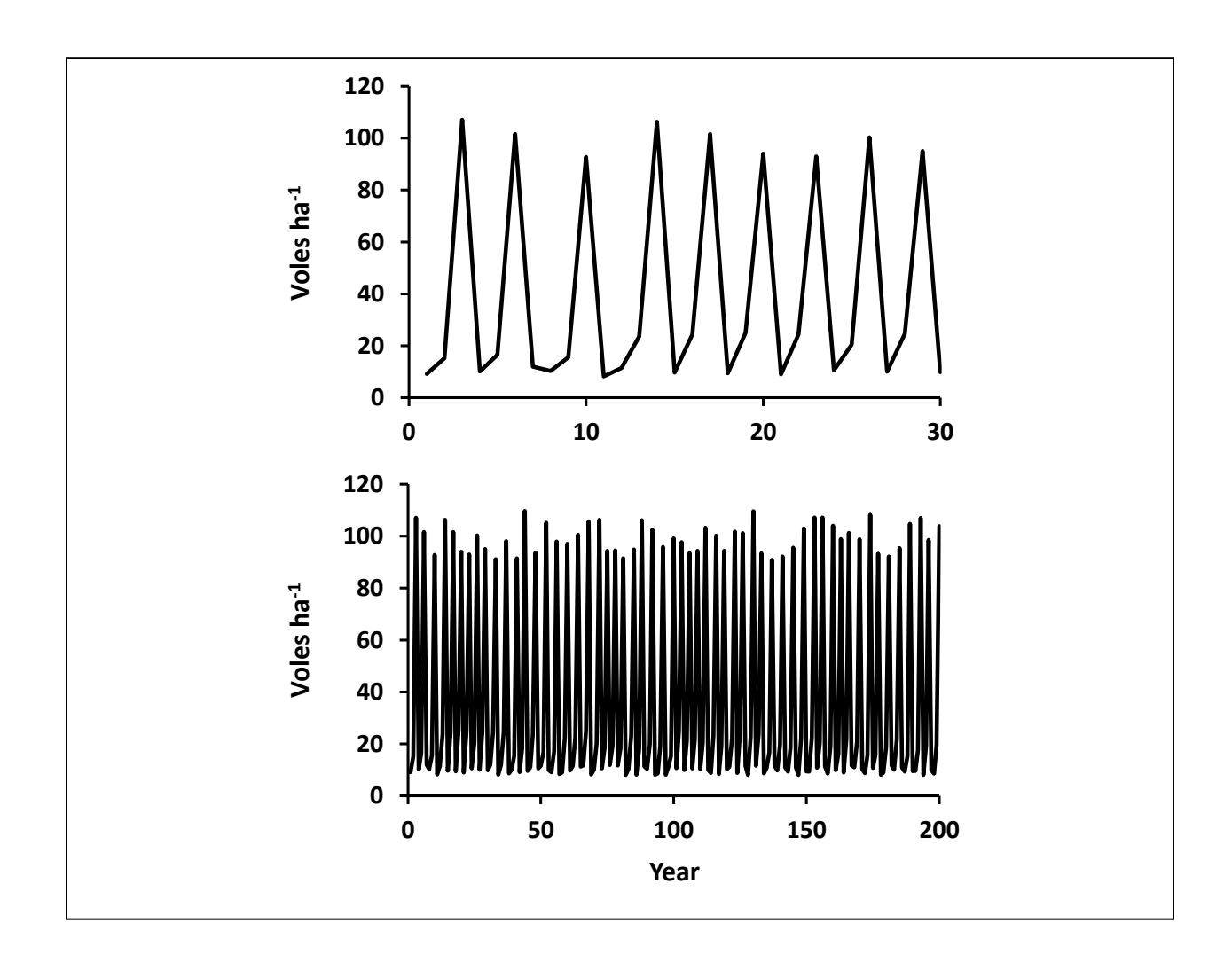
761

759 Figure 5: Simulated changes in plant, soil, and total ecosystem N with a linear increase in CO<sub>2</sub> from 400 to 800 µmol mol<sup>-1</sup> over 100 years, a linear warming from 10 to 15 °C over 100 years, 760 and both a linear increase in CO<sub>2</sub> from 400 to 800 µmol mol<sup>-1</sup> and a linear warming from 10 to 762 15 °C over 100 years (see Table 4). Different trajectories indicate responses with vole effects 763 aggregated with other biogeochemical processes (dotted black lines; simulations 5, 6, & 7), voles cycling between 8 and 110 voles ha<sup>-1</sup> on a three-to-four-year cycle (solid blue lines; simulations 765 8, 9, & 10), and a constant 100 voles ha<sup>-1</sup> (dashed red lines; simulations 11, 12, & 13).

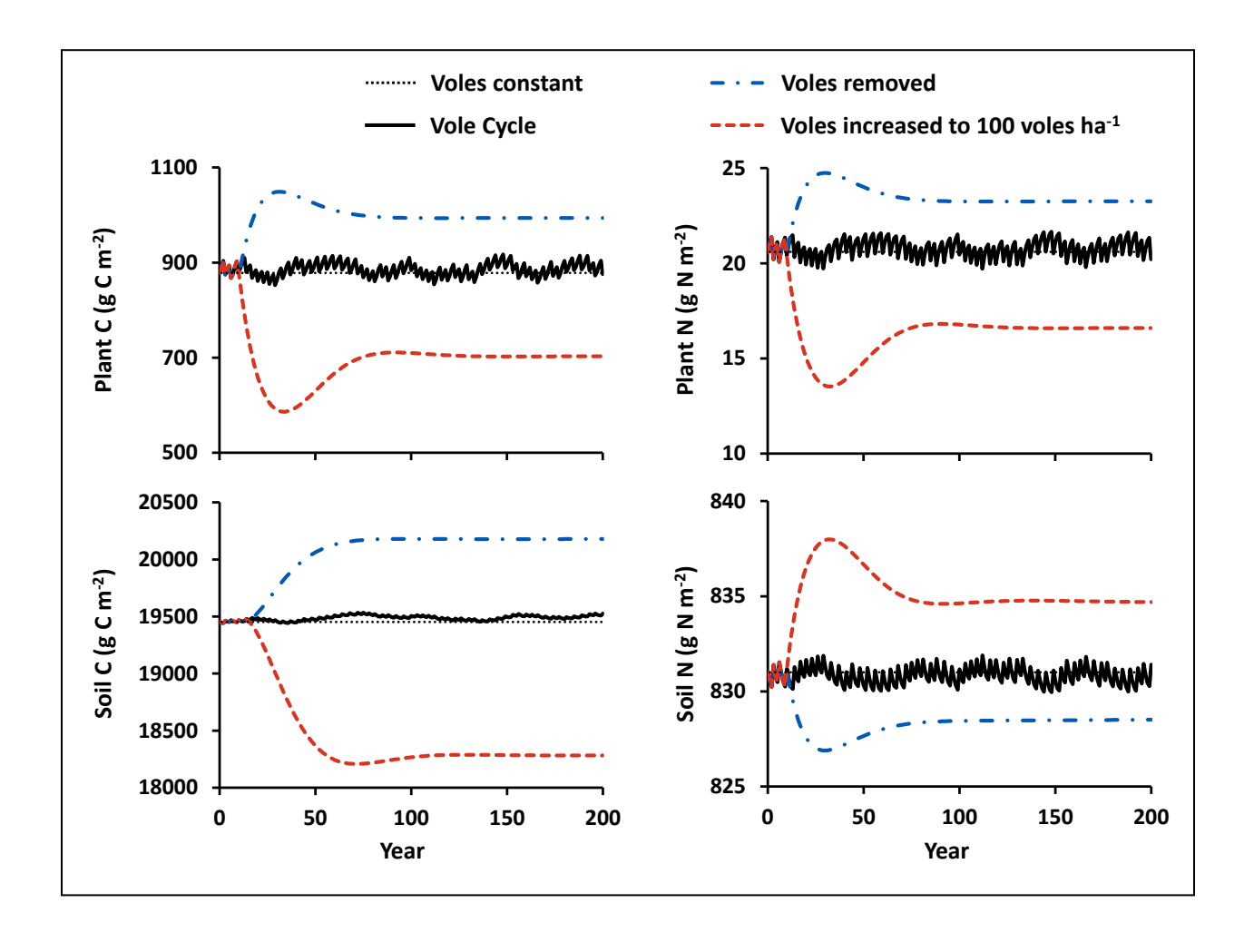
766

**Figure 6**: Simulated changes in gross primary (GPP), net primary (NPP), and net ecosystem production (NEP) with a linear increase in CO<sub>2</sub> from 400 to 800 μmol mol<sup>-1</sup> over 100 years, a linear warming from 10 to 15 °C over 100 years, and both a linear increase in CO<sub>2</sub> from 400 to 800 μmol mol<sup>-1</sup> and a linear warming from 10 to 15 °C over 100 years (see Table 4). Different trajectories indicate responses with vole effects aggregated with other biogeochemical processes (dotted black lines; simulations 5, 6, & 7), voles cycling between 8 and 110 voles ha<sup>-1</sup> on a three-to-four-year cycle (solid blue lines; simulations 8, 9, & 10), and a constant 100 voles ha<sup>-1</sup> (dashed red lines; simulations 11, 12, & 13).

**Figure 7**: Causal-chain diagram for the model in Box 1. Arrows indicate causal links: a red arrow marked with a "+" indicates that an increase in the variable at the tail of the arrow will cause an increase in the variable at the head of the arrow; a blue arrow marked with a "-" indicates that and increase in the variable at the tail of the arrow will cause a decrease in the variable at the head of the arrow. Symbols are defined in Table 1. Symbols in boxes are C and N stocks, symbols in circles are driver variables, and other symbols are either processes or allometric and stoichiometric constraints. The four causal links shown as dashed arrows are the links that were weakened in the calibration to accommodate vole-mediated processes in the simulations with explicit representation of vole density (see Table 2). The temperature (*T*) and vole (*V*) drivers are shown three times to avoid over complicating the diagram.

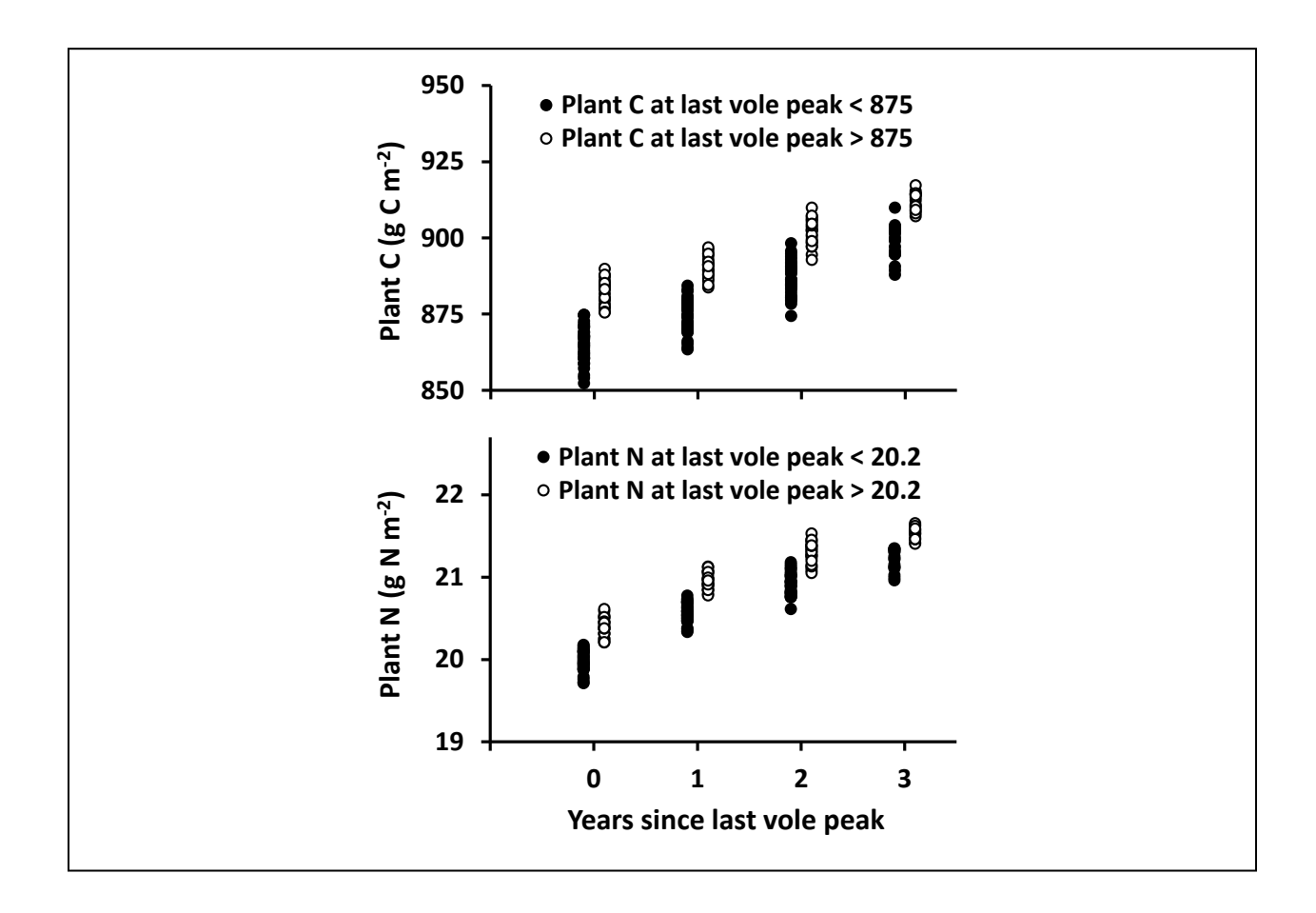


790 Figure 2791

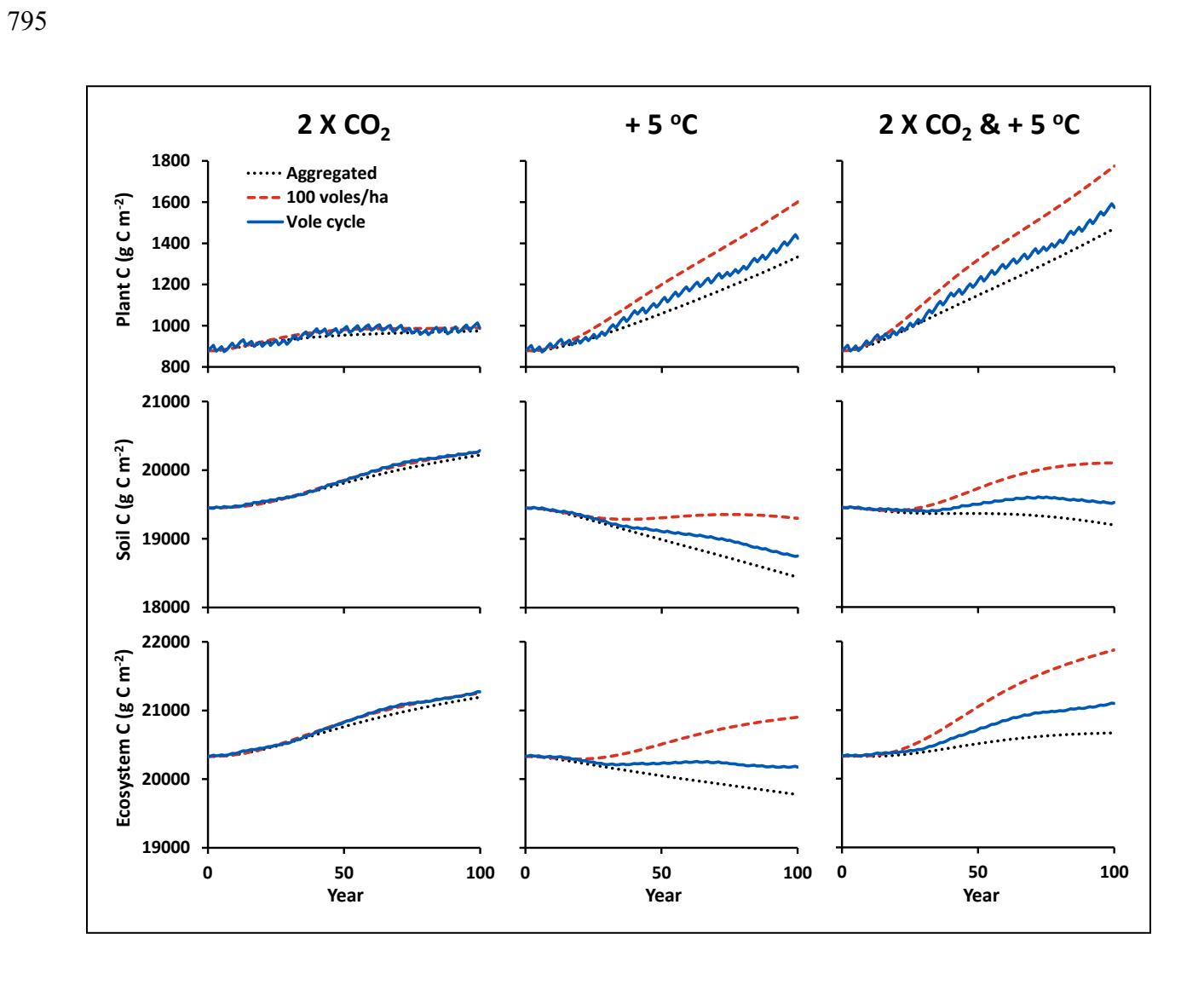


792 Figure 3

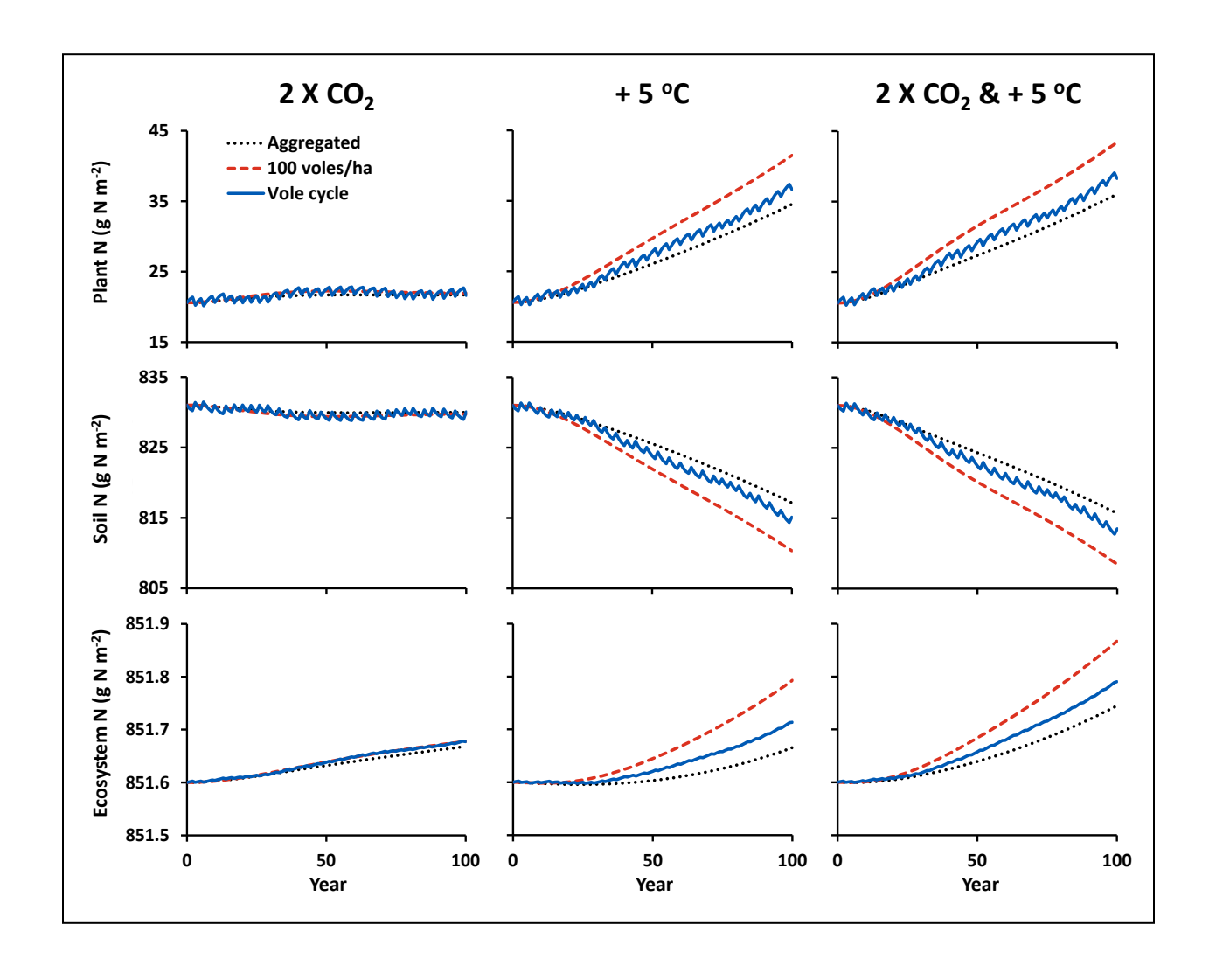


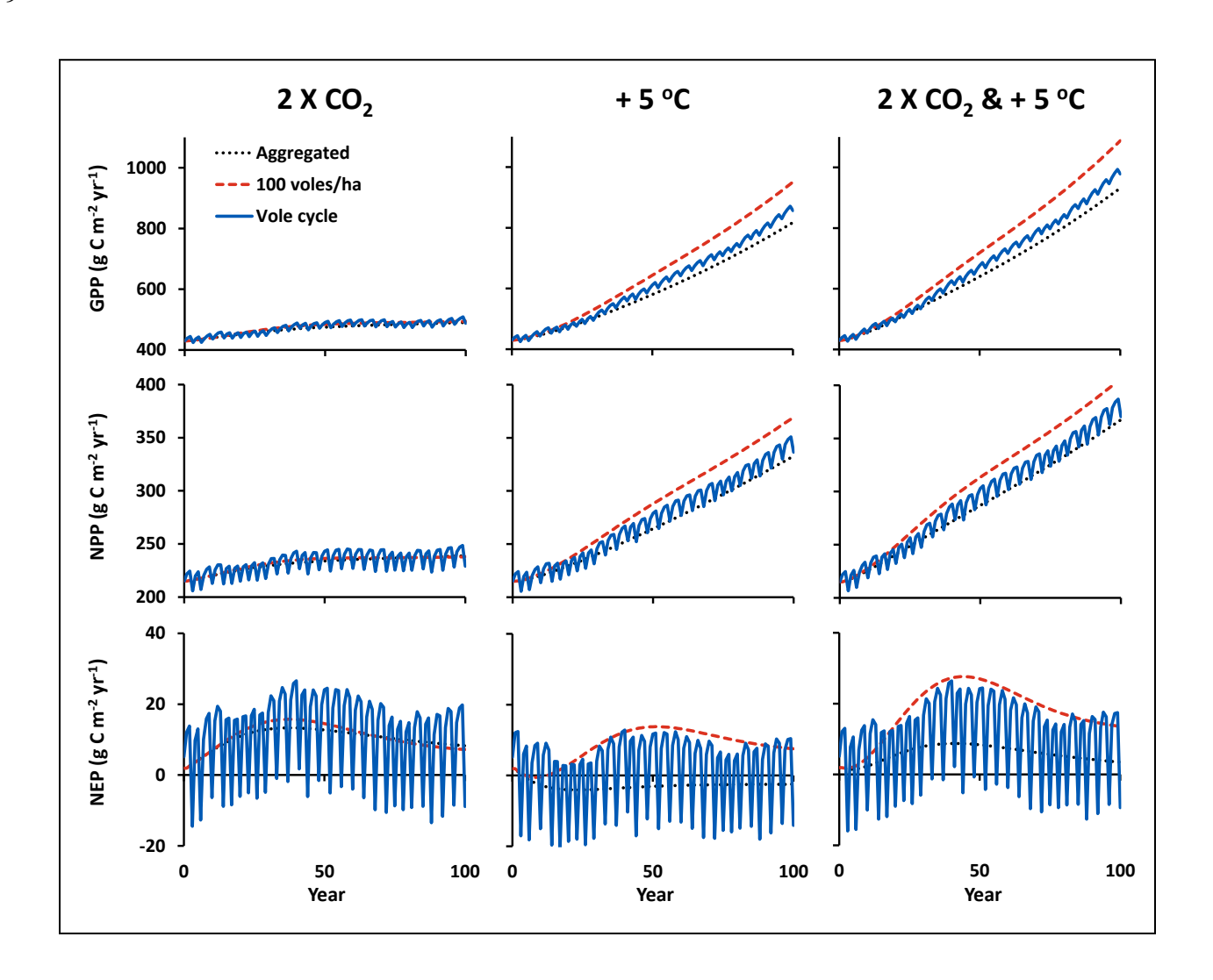


794 Figure 4

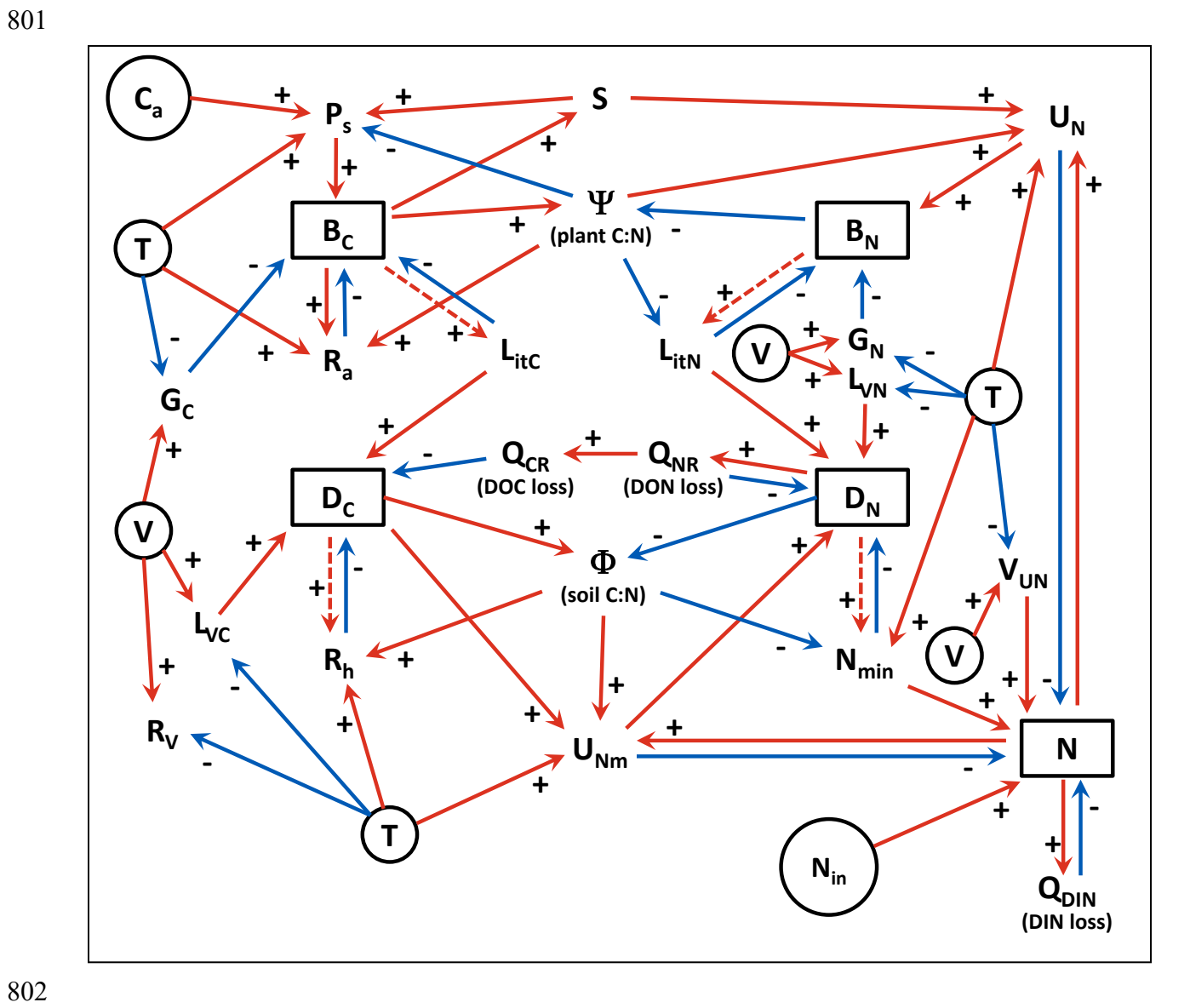


796 Figure 5797





800 Figure 7



Rastetter, E. B., K. L. Griffin, R. J. Rowe, L. Gough, J. R. McLaren, and N. T. Boelman. Model Responses to CO<sub>2</sub> and Warming Are Underestimated without Explicit Representation of Arctic Small-Mammal Grazing. Ecological Applications.

#### Appendix S1: Derivation of stocks, fluxes and parameter values.

### Section S1: Calibration for the aggregated model (vole activity not explicitly represented)

We set C and N stocks and fluxes to be consistent with data collated by Pearce et al. (2015) for the Multiple Element Limitation (MEL) model applied to tussock tundra (Table 2 in main text). Our detritus C and N are the aggregated value of the three detritus stocks the MEL model. To compensate for differences in model structures, we calculated litter-fall C and N ( $L_{itC}$  and  $L_{itN}$ ), heterotrophic respiration ( $R_h$ ), N immobilization ( $U_{Nm}$ ), and N inputs ( $N_{in}$ ) by difference assuming the ecosystem was in steady state.

We derived parameter values from various sources. We fit our allometric parameters ( $\alpha$  and  $\gamma$ ) to the MEL allometric equation for tundra from Pearce et al. (2015). We assume a stoichiometric balance for calibration and therefore set the optimum vegetation and detritus C:N ratios ( $q_B$  and  $q_D$ ) to the C:N ratios of the respective stocks from Pearce et al. (2015). Similarly, we set the C:N of dissolved organic matter losses ( $q_{DOM}$ ) to the ratio of the respective fluxes estimated from Pearce et al. (2015). To mimic the CO<sub>2</sub> response reported in Tissue and Oechell (1987), we set the CO<sub>2</sub> half-saturation constant for photosynthesis ( $k_C$ ) to 100  $\mu$ mol mol<sup>-1</sup>. To impose strong N limitation (Shaver et al. 2014), we set both the half saturation constants for plant ( $k_N$ ) and microbial ( $k_{Nm}$ ) N uptake to 1 g N m<sup>-2</sup> as in Rastetter et al. (2020).

We also set the temperature responses based on data from various sources. For photosynthesis we use a  $Q_{10}$  value of 1.55, which is a median of values derived from data in Tieszen (1973) and Rogers et al. (2019). For autotrophic respiration we use a  $Q_{10}$  of 2.7 based on a fit between 10 and 15 °C to the model for tundra species in Heskel et al. (2016). For heterotrophic respiration we use a  $Q_{10}$  of 3 again based on a fit between 10 and 15 °C to the model for Boreal forest soils in Carey et al. (2016). Atkin and Cummins (1994) report <sup>15</sup>N-based uptake rates for arctic plants consistent with  $Q_{10}$  values ranging from 1.16 to 3.17. Dong et al. (2001) and Yan et al. (2012) report plant N uptake rates in an agricultural setting consistent with  $Q_{10}$  values of 3.99 and 1.67. Based on these studies, we assume a  $Q_{10}$  of 2 for N uptake by plants. For microbial N uptake (immobilization), we use a  $Q_{10}$  value of 1.95 as reported by Roberts and Jones (2012) for microbial uptake of amino sugars. Finally, for N mineralization, Roberts and Jones (2012) report a  $Q_{10}$  value of 2.32 and Vinolas et al. (2001) report a value of 2; we use a  $Q_{10}$  value of 2.16.

Except for parameters associated with vole activity, the only parameters remaining are the rate parameters for each of the C and N fluxes. We calibrate these rate parameters to the process rates reported in Pearce et al. (2015) for the MEL model applied to tussock tundra (Table 2 in main text).

### Section S2:Calibration of the distributed model (explicit representation of vole activity)

We assume generic small mammals (voles and lemmings) weighing 50 g, but will refer to them as a "voles." We estimate C removal from vegetation by voles from two processes, consumption and nest building. The consumption rates depend on an allometric relation to body weight minus a correction for temperature to compensate for the energy needed to maintain body

the summer temperature we use to drive the model and subnivean temperature during the winter.

We assume that the average annual temperature experienced by the voles is ten degrees cooler than the average summer temperature:

854 
$$E = 26.82 + 5.36 W^{0.75} - 1.89 (T - 10)$$

where E is daily energy expenditure (kJ/vole/day), W is body weight (g fresh weight/vole), T is mean summer temperature ( ${}^{\circ}$ C). For a 50 g vole, this equation simplifies to

859 
$$E = 127.6 - 1.89 (T - 10)$$

Total food assimilation must meet this energy expenditure, but only about 33% of ingested forage gets assimilated (Batzli et al. 1980). Thus, total ingestion must contain about three times this amount of energy. To convert this ingestion to g C vole<sup>-1</sup> yr<sup>-1</sup>, we assume a forage energy density of 18.9 kJ/g dry weight (Batzli et al. 1980) and a C density of forage of 0.475 g C/g dry weight (Schlesinger 1991):

867 
$$I = 3512 - 52 (T - 10)$$

where I is ingestion (g C vole<sup>-1</sup> yr<sup>-1</sup>). Thus, for the ingestion part of Eq. 15 (Table 1 in main text)

871 
$$g_V = 3512 \text{ g C vole}^{-1} \text{ yr}^{-1}, \quad \varepsilon_V = 52 \text{ g C °C}^{-1} \text{ vole}^{-1} \text{ yr}^{-1}, \text{ and } T_0 = 10 \text{ °C}$$

Voles and lemmings also remove plant material to build winter nests. Vole nests contain about 20 g C nest<sup>-1</sup> (Rowe unpub. data). Krebs et al. (2012) estimate approximately 2.2 nests per lemming in the spring. Data from Maguire and Rowe (2017) indicate that singing vole density in spring is about half the average annual density. We therefore estimate that in addition to ingestion, our generic small mammal (vole) grazer removes 22 g C vole<sup>-1</sup> yr<sup>-1</sup> from the vegetation for nests. We add this nest C to the ingestion equation to get the final parameter for Eq. 15:

880 
$$n_V = 22 \text{ g C vole}^{-1} \text{ yr}^{-1}$$

Respiration is about 30% of ingestion (Batzli et al. 1980):

884 
$$r_V = 0.3 \text{ g C g}^{-1} \text{ C}$$

Forage contains about 25 mg N/g dry weight (Batzli et al. 1980), which is equivalent to a C:N ratio of 19 g C g<sup>-1</sup> N. We assume the C:N ratio of the nest material is the same as that of the vegetation (42.62 g C/g N). We calculate the C:N of material removed from vegetation by voles as the weighted mean of these two C:N ratios:

891 
$$q_V = \frac{3512 \times 19 + 22 \times 42.62}{3534} = 19.15 \text{ g C g}^{-1} \text{ N}$$

We set the per capita urine N production based on data for small mammals reported by Clark et al. (2005):

 $m_{NV} = 11 \text{ g N vole}^{-1} \text{ yr}^{-1}$ 896 897 898 899 **Section S3: LITERATURE CITED** 900 Atkin, O. K., and W. R. Cummins. 1994. The effect of root temperature on the induction of 901 nitrate reductase activities and nitrogen uptake rates in arctic plant species. Plant ans Soil 902 159:187-197. 903 Batzli, G. O., R. G. White, S. F. MacLean Jr, F. A. Pitelka, and B. D. Collier. 1980. The 904 herbivore-based trophic system. pp 335-410 in Brown, J., Miller, P.C., Tieszen, L.L., and 905 Brunnell, F.L. eds.. An Arctic Ecosystem: the Coastal Tundra at Barrow, Alaska. 906 Dowden, Hutchinson, and Ross Inc, Stroudsburg, PA, USA 907 Carey, J. C., J. Tang, P. H. Templar, K. D. Kroger, T. W. Crowther, A. J. Burton, J. S. Dukes, B. 908 Emmett, S. D. Frey, M. A. Heskel, L. Jiang, M. B. Machmuller, J. Mohan, A. M. 909 Panetta, P. B. Reich, S. Reinsch, X. Wang, S. D. Allison, C. Bamminger, S. Bridgham, S. 910 L. Collins, G. de Dato, W. C. Eddy, B. J. Enquist, M. Estiarte, J. Harte, A. Henderson, B. 911 R. Johnson, K. S. Larsen, Y. Luo, S. Marhan, J. M. Melillo, J. Peñuelas, L. Pfeifer-912 Meister, C. Poll, E. Rastetter, A. B. Reinmann, L. L. Reynolds, I. K. Schmidt, G. R. 913 Shaver, A. L. Strong, V. Suseela, and A. Tietema. 2016. Temperature response of soil 914 respiration largely unaltered with experimental warming. Proc Nat Accad Sci 113:13797-915 13802. 916 Clark, J. E., E. C. Hellgren, J. L. Parsons, E. E. Jorgensen, D. M. Engle, and D. M. Lesli Jr. 917 2005. Nitrogen outputs from fecal and urine deposition of small mammals: implications 918 for nitrogen cycling. Oecologia 144:447-455.

919 Dong, S., C. F. Scagel, L. Cheng, L. H. Fuchigami, and P. T. Rygiewicz. 2001. Soil temperature 920 and plant growth stage influence nitrogen uptake and amino acid concentration of apple 921 during early spring growth. Tree Phys. 21:541-547. 922 Heskel, M. A., O. S. O'Sullivan, P. B. Reich, M. G. Tjoelker, L. K. Weerasinghe, A. Penillard, J. 923 J. G. Egerton, D. Creek, K. J. Bloomfield, J. Xiang, F. Sinca, Z. R. Stangl, A. Martinez-924 de la Torre, K. L. Greffin, C. Huntingford, V. Hurry, P. Meir, M. H. Turnbull, and O. K. 925 Atkin. 2016. Convergence in the temperature response of leaf respiration across biomes 926 and plant functional types. Proc Nat Accad Sci 113: 3832-3837. 927 Krebs, C. J., F. Bilodeau, D. Reid, G. Gauthier, A. J. Kenney, S. Gilbert, D. Duchesne, and D. J. 928 Wilson. 2012. Are lemming winter nest counts a good index of population density? J 929 Mammalogy 93:87-92. 930 Maguire, A. J., and R. J. Rowe. 2017. Home range and habitat affinity of the singing vole on the 931 North Slope of Alaska. Arctic, Antarctic, and Alpine Research 492.:243–257. 932 Pearce, A. R., E. B. Rastetter, W. B. Bowden, M. C. Mack, Y. Jiang, Y., and B. L. Kwiatkowski, 933 B.L. 2015. Recovery of arctic tundra from thermal erosion disturbance is constrained by 934 nutrient accumulation: a modeling analysis. Ecological Applications 25:1271-1289. 935 Rastetter, E. B., G. W. Kling, G. R. Shaver, B. C. Crump, L. Gough, and K. L. Griffin. 2020. 936 Ecosystem recovery from disturbance is constrained by N cycle openness, vegetation-soil 937 N distribution, form of N losses, and the balance between vegetation and soil-microbial 938 processes. Ecosystems https://doi.org/10.1007/s10021-020-00542-3 939 Roberts. P., and D. L. Jones. 2012. Microbial and plant uptake of free amino sugars in grassland 940 soil. Soil Biology Biochemistry 49:139-149.

941	Rogers, A., S. P. Serbin, K. S. Ely, and S. D. Wullschleger. 2019. Terrestrial biosphere models
942	may overestimate arctic CO2 assimilation if they do not account for decreased quantum
943	yield and convexity at low temperature. New Phytologist 223:167-179.
944	Schlesinger, W. H. 1991. Biogeochemistry: An Analysis of Global Change. Academic Press, San
945	Diego, CA, USA.
946	Shaver, G. R., J. A. Laundre, M. S. Bret-Harte, F. S. Chapin, III, J. A. Mercado-Diaz, A. E.
947	Giblin, L. Gough, W. A. Gould, S. E. Hobbie, G. W. Kling, M. C. Mack, J. C. Moore, K.
948	J. Nadelhoffer, E. B. Rastetter, and J. P. Schimel, J.P. 2014. Terrestrial Ecosystems at
949	Toolik Lake, Alaska. In Hobbie, J.E., and G. W. Kling (eds.). A Changing Arctic:
950	Ecological Consequences for Tundra, Streams and Lakes. Oxford University Press, New
951	York, NY, USA.
952	Tieszen, L. L. 1973. Photosynthesis and respiration in arctic tundra grasses: field light intensity
953	and temperature responses. Arctic Alpine Res 5:239-251.
954	Tissue, D. T., and W. C. Oechell. 1987. Response of Eriophorum vaginatum to elevated CO2
955	and temperature in the Alaskan tussock tundra. Ecology 68:401-410.
956	Vinolas, L. C., V. R. Vallejo, and D. L. Jones. 2001. Control of aminoacid mineralization and
957	microbial metabolism by temperature. Soil Biology Biochemistry 33:1137-1140.
958	Yan, Q., Z. Duan, J. Mao, X. Li, and F. Dong. 2012. Effects of root-zone temperature and N, P,
959	and K supplies on nutrient uptake of cucumber Cucumis sativus L seedlings in
960	hydroponics. Soil Science and Pland Nutrition 58:707-717.
961	
962	